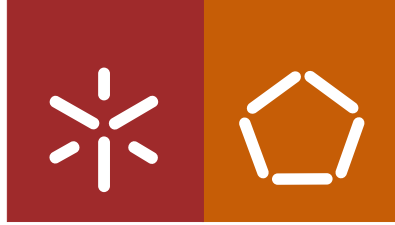




Universidade do Minho
Escola de Engenharia

Andréa Teixeira Pimenta Marinho

**Modification of chitosan based
membranes with polydopamine**



Universidade do Minho
Escola de Engenharia

Andréa Teixeira Pimenta Marinho

**Modification of chitosan based
membranes with polydopamine**

Dissertação de Mestrado
Mestrado em Propriedades e Tecnologias de Polímeros

Trabalho efetuado sob a orientação da
Professora Doutora Natália Alves

outubro de 2015

Declaração

Nome: Andréa Teixeira Pimenta Marinho

Endereço eletrónico: andrepimenta@live.com.pt

Título dissertação: Modification of chitosan based membranes with polydopamine

Orientadora: Professora Doutora Natália Alves

Ano de Conclusão: 2015

Designação do Mestrado: Mestrado em Propriedades e Tecnologias de Polímeros

DE ACORDO COM A LEGISLAÇÃO EM VIGOR, NÃO É PERMITIDA A REPRODUÇÃO DE QUALQUER PARTE DESTA DISSERTAÇÃO.

Universidade do Minho, ___/___/_____

Assinatura: _____

Acknowledgements

First of all, I would like to thank Professor Natália for all the support and trust deposited in accepting guiding me in this project

I also want to thank Catarina Vale and Sofia Caridade for all the help in the laboratory. Thank you to Professor Gabriela Botelho and Daniela Correia of chemistry department of Minho University for all the help and availability.

Thank you too to Engineer Maurício Malheiro from department of Polymer Engineering of Minho University for the support in the realization of FTIR tests.

To my friends Cristina Costa and Carolina Macedo a special thanks, for their support and encouragement over these months of work.

And finally, a huge thank you to my family for all the help and comprehension during this work.

To all those who directly or indirectly contributed to this work, thank you very much!

Abstract

In a marine environment, specific proteins are secreted by mussels which work as a glue, allowing the mussels become strongly attached to rocks, and thus resist to the harsh marine conditions. Mussel adhesive proteins (MAPs) present an unusual amino acid 3, 4-dihydroxyphenylalanine (DOPA), and their outstanding adhesive properties have been attributed to the presence of the catechol groups presents in this amino acid.

Inspired by the chemical composition of MAPs, chitosan based membranes were successfully modified with polydopamine in the present work. It was shown that dopamine formed a self-polymerized coating in both chitosan membranes crosslinked with the natural agent genipin and non-crosslinked chitosan membranes.

The modified membranes were characterized by Proton Nuclear Magnetic Resonance (¹H-NMR), Ultraviolet Visible Spectrophotometry (UV-Vis), Fourier Transform Infrared Spectrophotometry (FTIR), Scanning Electron Microscopy (SEM), AFM and contact angles measurements. Finally, adhesion tests were performed on pigskin.

The modification of chitosan based membranes with dopamine allowed to enhance their adhesive properties. The developed membranes could be potentially used in skin wound healing.

Resumo

No ambiente marinho, proteínas específicas são segregadas por mexilhões, que funcionam como uma cola, permitindo que os mexilhões se prendam fortemente às rochas, e assim resistam às condições marinhas adversas. As proteínas adesivas dos mexilhões (MAPs) apresentam um aminoácido invulgar, o dihidróxidofenilalanina (DOPA), e as suas excelentes propriedades têm sido atribuídas à presença do grupo catecol presente neste aminoácido.

Inspirados pela composição química das proteínas segregadas pelos mexilhões, neste trabalho, a modificação de membranas à base de quitosano com polidopamina, foi efetuada com sucesso. Verificou-se que a dopamina forma um revestimento autopolimerizado em ambas as membranas, reticuladas e não-reticuladas com o agente natural genipin.

As membranas modificadas foram caracterizadas por Ressonância Magnética Nuclear de Protão (H-NMR), Espectroscopia Ultravioleta – Visível (UV-Vis), Espectroscopia de Infravermelho por Transformada de Fourier (FTIR), Microscopia Eletrónica de Varrimento (SEM), AFM e testes de medição de ângulos de contacto. Por último, foram efetuados testes de adesão em pele de porco.

Através do revestimento das membranas de quitosano com a polidopamina, foram melhoradas as suas propriedades adesivas, evidenciando forte potencialidade de serem utilizadas em aplicações biomédicas, nomeadamente no tratamento de feridas cutâneas.

Contents

Acknowledgements	iii
Abstract.....	iv
Resumo	v
Contents	vi
List of abbreviations	viii
List of figures	ix
List of tables	x
Chapter 1 Introduction.....	11
1.1 Motivation and content	11
1.2 Biodegradable Polymers for Biomedical Applications	12
1.3 Materials Modification with Polydopamine	14
References.....	17
Chapter 2 - Materials and Methods	19
2.1 Materials	19
2.1.1 Chitosan.....	19
2.1.2 Genipin	20
2.1.3 Dopamine	21
2.2 Methods	22
2.2.1 Production of chitosan films	22
2.2.2 Coating of the films with polydopamine.....	23
2.2.3 Characterization techniques	24
2.2.3.1 Fourier Transform Infrared Spectroscopy (FTIR)	24
2.2.3.2 Ultraviolet spectrometry (UV-Vis)	25
2.2.3.3 Proton Nuclear Magnetic Resonance (H-NMR).....	26
2.2.3.4 Scanning Electron Microscopy (SEM)	27

2.2.3.5 Atomic force microscopy (AFM) coupled with nanoindentation tests	28
2.2.3.6 Water Contact angle measurement.....	29
2.2.3.7 Bioadhesion tests.....	30
References.....	32
Chapter 3 - Modification of chitosan based membranes with polydopamine	35
Abstract.....	35
3.1 Introduction.....	35
3.2 Experimental.....	38
3.2.1 Materials.....	38
3.2.2 Production of chitosan membranes	38
3.2.3 Polydopamine coatings on the uncrosslinked and crosslinked membranes..	39
3.2.4 Characterization of the produced membranes	39
3.2.4.1 UV-Visible spectroscopy (UV-Vis) measurements	39
3.2.4.2 Scanning Electron Microscopy (SEM) and Atomic force microscopy (AFM).....	39
3.2.4.3 Water contact angle measurements (WCA)	39
3.2.4.4 Bioadhesion tests.....	40
3.3 Results and Discussion	40
3.3.1 UV-Visible spectroscopy (UV-Vis).....	40
3.3.2 Water contact angle measurements	42
3.3.3 Scanning Electron Microscopy (SEM) and Atomic force microscopy (AFM)	44
3.3.4 Bioadhesion tests.....	46
3.4 Conclusions.....	47
References.....	48
Chapter 4 - Concluding remarks.....	51
Annex.....	52

List of abbreviations

A

AFM- Atomic Force Microscopy

ASTM- American Society for Testing and Materials

ATR- Attenuated Total Reflection

Au- Gold

C

C- Carbon

CHT- Chitosan

D

DD- Degree of deacetylation

DOPA - 3, 4-dihydroxyphenylalanine

F

FTIR- Fourier Transform Infrared Spectroscopy

G

GAGs- Glycosaminoglycans

GP- Genipin

H

HA- Hyaluronic Acid

I

IR- Infrared

L

LbL- Layer by Layer

M

MAPs- mussel adhesive proteins

mrMAP- DOPA-containing recombinant Mussel Adhesive Protein

N

NMR- Nuclear Magnetic Resonance spectroscopy

P

PCL- Polycaprolactone

PDA- Polydopamine

R

Rq- Root mean square

Ra- Average roughness

S

SEM- Scanning Electron Microscopy

U

UV-Vis- Ultraviolet-Visible spectrophotometry

W

WCA- Water contact angle measurements

List of figures

Figure 1.1- Schematic illustration of cell adhesion on substrates modified by mussel-inspired polydopamine. Adapted from [9]	11
Figure 1.2 - Schematic diagram of tissue engineering. Osteoblasts (bone cells), chondrocytes (cartilage cells), hepatocytes (liver cells), enterocytes (intestinal cells), and urothelial cells are depicted. Adapted from [13].	13
Figure 1.3- Immobilization and pH- responsive release of dox from PDA capsules. The red dots represent Dox. Adapted from [21].	15
Figure 1.4-Schematic representation of tissue adhesive hydrogels. Adapted from [27]	16
Figure 2.1 - Deacetylation of chitin. Adapted from [30].	19
Figure 2.2 - Schematic of genipin chemical structure. Adapted from [38].	21
Figure 2.3 - Dopamine polymerization. Adapted from [44].	21
Figure 2.4 - Schematic representation of the crosslinking reaction chitosan with genipin. Adapted from [38.]	22
Figure 2.5 - Drying process of a chitosan film.	23
Figure 2.6 - Dopamine coating films.	24
Figure 2.7 - a) Scheme of a typical force versus the AFM tip displacement acquired in indentation of a surface. b) States of the AFM probe corresponding to the three points figured on the force curve. Adapted from [56].	28
Figure 2.8- General illustration of contact angle formed by sessile liquid drops. Adapted from [58].	29
Figure 2.9- Equipment used to performed adhesion tests and their schematic illustration. Where ΔL is the displacement of top vice and A_0 is the overlapping area.	31
Figure 3.1 - Image of a membrane before and after coating.	40

- Figure 3.2- UV-Vis spectra of the CHT (blue) and crosslinked CHT membranes at different crosslinking degrees: 0.1 % (orange); 1 % (grey); and 2 % (yellow) of GP. ... 41
- Figure 3.3- UV-Vis spectra of a) non-crosslinked CHT and non-crosslinked CHT modified with PDA membrane; b) 0.1 % crosslinked CHT and 0.1 % crosslinked CHT modified with PDA membrane; c) 1% crosslinked CHT and 1 % crosslinked CHT modified with PDA membrane and d) 2% crosslinked CHT and 2% crosslinked modified with PDA membrane. 42
- Figure 3.4- Relation between absorbance and crosslinking degree for the PDA coated membranes..... 42
- Figure 3.5- WCA measurements of unmodified (blue bars) and modified CHT membranes with PDA (orange bars). 43
- Figure 3.6- Representative SEM images of- a) CHT membranes; b) modified CHT membranes; c) 0.1% crosslinked CHT membranes; d) modified 0.1% crosslinked CHT membranes; e) 1% crosslinked CHT membranes; f) modified 1% crosslinked CHT membranes; g) 2% crosslinked CHT membranes and h) modified 2% crosslinked CHT membranes..... 44
- Figure 3.7- Representative AFM images ($5\mu\text{m} \times 5\mu\text{m}$) of- a) CHT membranes; b) modified CHT membranes; c) 2% crosslinked CHT membranes and d) modified 2% crosslinked CHT membranes. Rq and Ra values of the studied surfaces..... 45
- Figure 3.8- Young's Modulus and adhesion force of unmodified (blue bars) and modified (orange bars) 2% crosslinked CHT membranes determined by AFM. 46
- Figure 3.9- Tensile tests performed according ASTM D1002: Adhesion strength for both unmodified (blue bars) and modified (orange bars) 2% crosslinked membranes. 47

List of tables

- Table 2.1- Hydrophilic and hydrophobic character depending on the contact angle value. Adapted from [60]..... 29

Chapter 1 Introduction

1.1 Motivation and content

Over the last years, several attempts have been made to replace petrochemical products by renewable natural sources components. Polymers that exist in abundance in nature such as starch, collagen, gelatin, cellulose, alginate and chitin represent attractive candidates because they might reduce the current dependency on fossil fuels and, consequently, have a positive environment impact¹. The most challenging part of this approach is to obtain bio-based materials with properties equivalent to those of fully synthetic products. That way, biopolymer membranes are becoming more and more compelling due their growing demand in environment, energy and healthy fields².

The marine environment is filled with bioactive natural products, many of which exhibit characteristics that are not found in terrestrial natural products³. In a marine environment, mussels secrete specific proteins that are used as a biological glue which generate a strong bond with the surface, thus being capable of surviving to the destructive conditions of the ocean⁴. This outstanding mussel adhesive power is due to the presence of 3,4- dihydroxyphenylalanine (DOPA), an amino acid formed by posttranslational modification of tyrosine^{5,6}. Lee *et al*⁷ hypothesized that the coexistence of catechol and amine groups in mussels is crucial for achieving adhesion to different material surfaces. Thereafter they identified dopamine as a small-molecule that contains both functionalities, and that is useful for the surface modifications of many materials such polymers, metals and ceramics^{7,8}- Figure 1.1.

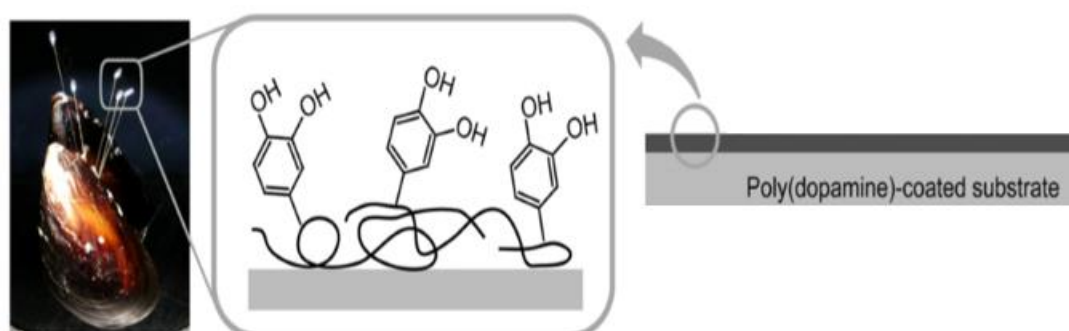


Figure 1.1- Schematic illustration of cell adhesion on substrates modified by mussel-inspired polydopamine. Adapted from [9].

Inspired by the chemical composition of the adhesive proteins in mussels, chitosan films were coated with polydopamine in the present work, which could be potentially used in skin wound healing, in the form of bioadhesives.

The present chapter will provide an overview of the use of biodegradable polymers, such as chitosan, as biomaterials and their importance and applicability in the biomedical field, especially in tissue engineering. A review of the main works where polydopamine has been used to coat distinct substrates, will also be presented. The materials and methods used in this work will be described in chapter 2. The results will be presented and discussed in chapter 3, and in chapter 4 shall be provided the conclusions and general comments of the work.

1.2 Biodegradable Polymers for Biomedical Applications

The use of biomaterials has significantly impacted the advancement of modern medicine⁹. During the last two decades significant advances have been made in the development of different biodegradable polymeric materials for various biomedical applications¹⁰.

A biomaterial can be defined as any natural or synthetic substance engineered to interface with biological systems to evaluate, augment, treat or replace any tissue, organ or function of the body^{9,11}. So, the main requisite to qualify a material as a biomaterial is that it should be biocompatible. The main type of biomaterials are biopolymers: biopolymers can be classified into biodegradable and non-biodegradable biopolymers, according to their degradation properties.

The most important properties of biodegradable biomaterials are as follows¹⁰:

(1) The material should have acceptable shelf life, (2) The material should not cause an inflammatory or toxic response upon implantation in the body, (3) The material should have appropriate mechanical properties for the indicated application and the variation in mechanical properties with degradation should be compatible with the healing or regeneration process, (4) The degradation time of the material should match the healing or the regeneration process, (5) The degradation products should be non-toxic and able to get metabolized and cleared from the organism.

Biodegradable polymers are of utmost interest because these materials are able to be broken down and excreted or resorbed without removal or surgical revision⁹.

Therefore, today biodegradable polymeric materials have had applications as: large implants such as bone screws, bone plates and contraceptive reservoirs; small implants, such as staples, sutures and nano or micro-sized drug delivery vehicles; plain membranes for guided tissue regeneration and multifilament meshes or porous structures for tissue engineering¹⁰. The purpose of the present work is to develop biodegradable membranes that could be used in tissue engineering.

Tissue engineering, which applies methods of engineering and life sciences to create artificial constructions for the regeneration tissue (Figure 1.2), has recently attracted the scientist and medical community in hopes of getting less invasive and painful treatments for patients^{12,13}. A fascinating characteristic of tissue engineering is to regenerate patient's own tissue or organ that are entirely free of poor biocompatibility as well as a severe immune rejection¹⁴.

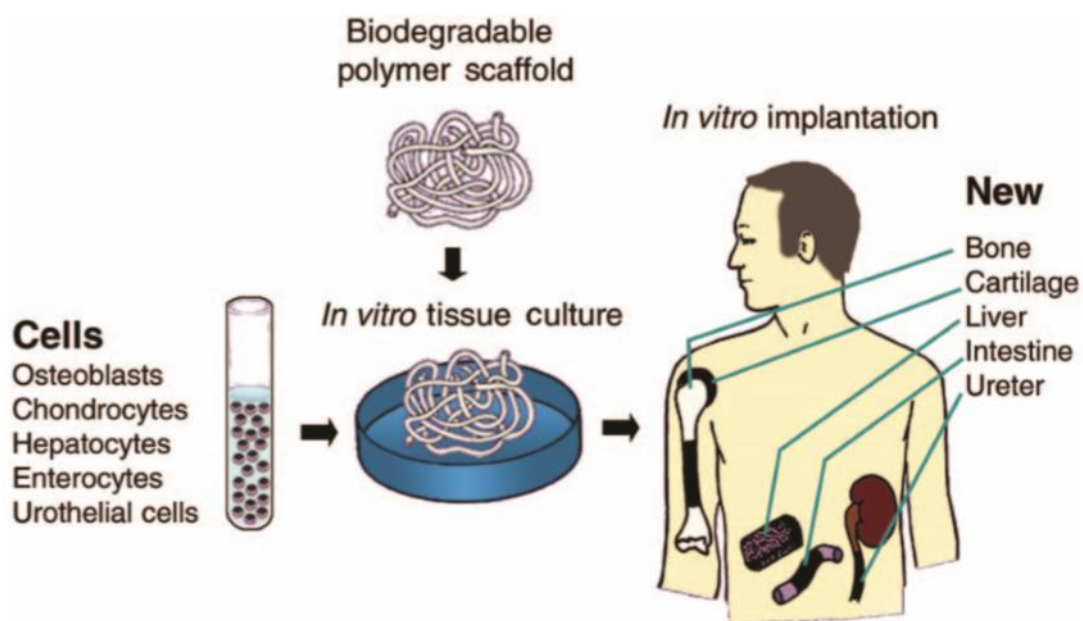


Figure 1.2 - Schematic diagram of tissue engineering. Osteoblasts (bone cells), chondrocytes (cartilage cells), hepatocytes (liver cells), enterocytes (intestinal cells), and urothelial cells are depicted. Adapted from [13].

As depicted in Figure 1.2, commonly, cells are implanted into an artificial structure able of supporting three-dimensional tissue formation, these structures are typically named as scaffolds. Scaffolds should have mechanical properties similar those of the tissue at the implantation site, exhibit biocompatibility, low toxicity profiles and have the ability to support cell growth and proliferation¹⁵. Scaffolds must preferentially be absorbed by the surrounding tissues (without the necessity of to perform a surgery removal), so biodegradability is an essential factor. The material must degrade to non-

toxic products, within the time frame required for the application. The first tissue successfully engineered in laboratory was skin¹⁶.

Biopolymers as biomaterials in tissue engineering are very important once they offer important options in control of structure, morphology and chemistry as reasonable substitutes. Even the intrinsic biodegradability of biopolymers is important to help to moderate the rate and de extent of cell and tissue remodeling in vitro or in vivo¹⁷. As well as the primary function, to provide structural support, it is also wanted that the biomaterial promote and maintain an environment that enables an appropriate cell adhesion, growth and differentiation, in order to lead to new tissue formation and the required function.

A good example of a biopolymer used in tissue engineering is chitosan, the base compound used in the present work. Chitosan is structurally similar to glycosaminoglycans (GAGs), found in the extracellular matrix of several human tissues¹⁸. CHT can act as a wound dressing as it exhibits a positive charge, mild gelation characteristics, film forming capacity and tissue-adhesiveness¹³. It accelerates wound healing by improving the functions of inflammatory cells¹⁴.

1.3 Materials Modification with Polydopamine

Polydopamine (PDA) has been used by some authors to modify distinct substrates, envisaging tissue engineering applications. For example, Park *et al*¹⁹ have functionalized the surface of polycaprolactone (PCL) nanofibers with a PDA ad-layer to enhance the attachment and proliferation of endothelial cells as a potential application in vascular tissue engineering. PDA is undoubtedly a promising tool in the biomedical field because in addition to its adhesive properties, it is biocompatible and demonstrates negligible toxicity to cells as shown by Posta and co-workers²⁰. They coated silica (SiO₂) particles with PDA and biocompatibility tests have demonstrated negligible toxicity of the particles to cells, making them promising for drug delivery applications²⁰. PDA has also been used in capsules for drug delivery because of their ability to be functionalized. To explain in more detail how this process occurs, Caruso *et al* work²¹ is shortly described. They have reported a facile approach to immobilize a pH-cleavable polymer-drug conjugate within PDA capsules for intracellular delivery of an anticancer drug²¹. The anticancer drug doxorubicin (Dox) was conjugated to thiolated poly (methacrylic acid) (PMA_{SH}) and immobilized in PDA capsules - Figure 1.3.

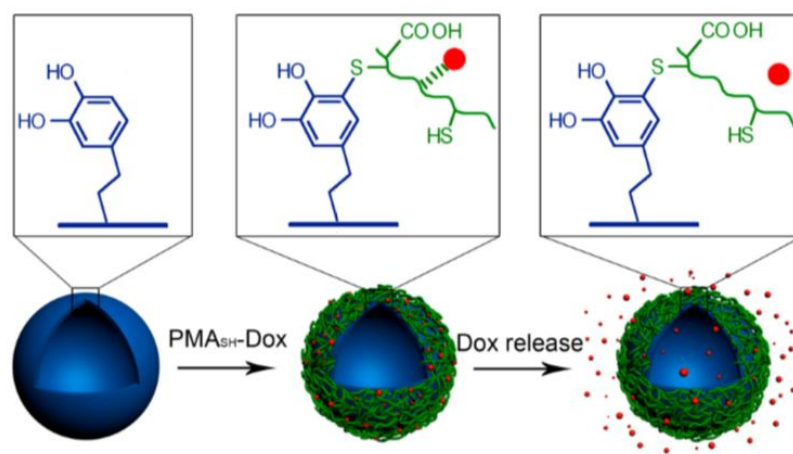


Figure 1.3- Immobilization and pH- responsive release of dox from PDA capsules. The red dots represent Dox. Adapted from [21].

The polymer-drug conjugate (PMA_{SH}-Dox) was loaded in polydopamine capsules via thiol-catechol reactions (between the conjugate and capsule walls). Finally, the anticancer drug is released from the drug-loaded PDA capsules when the pH-response occurs. These PDA capsules showed pH-responsive drug release behavior and enhanced anticancer efficacy compared with free drugs.

It has been shown that the catechol groups are the key aspect of polydopamine, responsible for the enhanced adhesion and playing a versatile and important role in the design of coatings and bioadhesives²². Compared with synthetic adhesives, bioadhesives in many living systems are known for their superior strength and good biocompatibility, they are therefore considered promising biomaterials for use in biomedical and tissue engineering^{23,24}.

There has been an acceptance for the application of bioadhesives for human tissue regeneration as an alternative to sutures, as they carry numerous advantages. They can be used in external or internal lacerations, and surgical incisions allowing an easy, fast and non-invasive procedure and can be applied in parts where suturing is impossible²⁵.

Neto and co-workers²⁶ have produced multilayer films layer-by-layer (LbL) technique using chitosan and dopamine modified hyaluronic acid, in order to try to combine the adhesion properties found in marine mussels with a simple film production method. The evaluation of cell behavior demonstrated that films present an enhanced cell adhesion, proliferation and viability. Making that these films could be potentially used as adhesive coating of distinct implants, in order to improve both cell response and adhesion strength in a simple and versatile way.

Ryu et al²⁷ have developed robust tissue adhesive hydrogels consisting of catechol-functionalized chitosan and thiol-terminated Pluronic. These thermosensitive, injectable

and tissue adhesive hydrogels showed excellent mechanical properties and stability in vitro and in vivo. They were able to form immediately adhesive gels to the tissue after injection – Figure 1.4, holding high potential for medical applications like arresting bleeding²⁷.

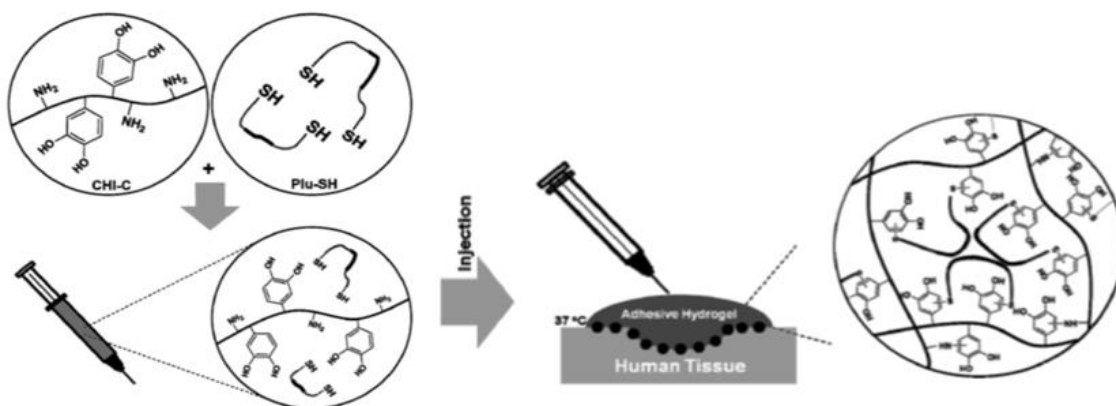


Figure 1.4-Schematic representation of tissue adhesive hydrogels. Adapted from [27].

Very recently, Kim et al²⁸ proposed a bioadhesive which could be used as a promising sealant for urinary fistula. To obtain water-immiscible mussel protein based bioadhesive (WIMBA), a complex coacervate was formed between DOPA-containing recombinant mussel adhesive protein (mrMAP) and hyaluronic acid (HA) in aqueous condition. WIMBA satisfied two essential requirements: water resistance and high adhesion strength. The tests were performed in rats and the developed water-immiscible mussel protein based bioadhesive successfully sealed punctured bladders and withstood intravesical pressure to prevent incontinence²⁸.

References

1. Croisier, F. & Jérôme, C. Chitosan-based biomaterials for tissue engineering. *Eur. Polym. J.* **49**, 780–792 (2013).
2. Yang, H.-C., Luo, J., Lv, Y., Shen, P. & Xu, Z.-K. Surface engineering of polymer membranes via mussel-inspired chemistry. *J. Memb. Sci.* **483**, 42–59 (2015).
3. Carté, B. K. Biomedical potential of marine natural products. *Bioscience* **46**, 271–286 (1996).
4. Lee, B. P., Dalsin, J. L. & Messersmith, P. B. Synthesis and Gelation of DOPA-Modified Poly (ethylene glycol) Hydrogels. 1038–1047 (2002).
5. Murphy, J. L., Vollenweider, L., Xu, F. & Lee, B. P. Adhesive performance of biomimetic adhesive-coated biologic scaffolds. *Biomacromolecules* **11**, 2976–2984 (2010).
6. Dalsin, J. L., Hu, B. H., Lee, B. P. & Messersmith, P. B. Mussel adhesive protein mimetic polymers for the preparation of nonfouling surfaces. *J. Am. Chem. Soc.* **125**, 4253–4258 (2003).
7. Lee, H., Dellatore, S. M., Miller, W. M. & Messersmith, P. B. Mussel-inspired surface chemistry for multifunctional coatings. *Science* **318**, 426–430 (2007).
8. Kang, J. *et al.* Immobilization of bone morphogenetic protein on DOPA- or dopamine-treated titanium surfaces to enhance osseointegration. *Biomed Res. Int.* **2013**, (2013).
9. Ulery, B. D., Nair, L. S. & Laurencin, C. T. Biomedical applications of biodegradable polymers. *J. Polym. Sci. Part B Polym. Phys.* **49**, 832–864 (2011).
10. Nair, L. S. & Laurencin, C. T. Biodegradable polymers as biomaterials. *Prog. Polym. Sci.* **32**, 762–798 (2007).
11. Tian, H., Tang, Z., Zhuang, X., Chen, X. & Jing, X. Biodegradable synthetic polymers: Preparation, functionalization and biomedical application. *Prog. Polym. Sci.* **37**, 237–280 (2012).
12. Ma, P. X. Biomimetic materials for tissue engineering. *Advanced Drug Delivery Reviews* **60**, 184–198 (2008).
13. Langer, R. Biomaterials for Drug Delivery and Tissue Engineering. **31**, 477–485 (2006).
14. Hetal Patel*, Minal Bonde, G. S. D. Biodegradable polymer scaffolds for tissue engineering. *Trends Biomater. Artif. Organs* **25**, 20–29 (2011).

15. Gunatillake, P. a., Adhikari, R. & Gadegaard, N. Biodegradable synthetic polymers for tissue engineering. *Eur. Cells Mater.* **5**, 1–16 (2003).
16. Chen, M., Przyborowski, M. & Berthiaume, F. Stem cells for skin tissue engineering and wound healing. *Crit. Rev. Biomed. Eng.* **37**, 399–421 (2009).
17. Velema, J. & Kaplan, D. Biopolymer-based biomaterials as scaffolds for tissue engineering. *Advances in Biochemical Engineering/Biotechnology* **102**, 187–238 (2006).
18. Sophia Fox, A. J., Bedi, A. & Rodeo, S. a. The basic science of articular cartilage: structure, composition, and function. *Sports Health* **1**, 461–8 (2009).
19. Ku, S. H. & Park, C. B. Human endothelial cell growth on mussel-inspired nanofiber scaffold for vascular tissue engineering. *Biomaterials* **31**, 9431–9437 (2010).
20. Postma, A. *et al.* Self-polymerization of dopamine as a versatile and robust technique to prepare polymer capsules. *Chem. Mater.* **21**, 3042–3044 (2009).
21. Cui, J. *et al.* Immobilization and intracellular delivery of an anticancer drug using mussel-inspired polydopamine capsules. *Biomacromolecules* **13**, 2225–2228 (2012).
22. Faure, E. *et al.* Catechols as versatile platforms in polymer chemistry. *Prog. Polym. Sci.* **38**, 236–270 (2013).
23. Lim, S., Choi, Y. S., Kang, D. G., Song, Y. H. & Cha, H. J. The adhesive properties of coacervated recombinant hybrid mussel adhesive proteins. *Biomaterials* **31**, 3715–3722 (2010).
24. Xue, J., Wang, T., Nie, J. & Yang, D. Preparation and characterization of a photocrosslinkable bioadhesive inspired by marine mussel. *J. Photochem. Photobiol. B Biol.* **119**, 31–36 (2013).
25. Marques, D. S. *et al.* Photocurable bioadhesive based on lactic acid. *Mater. Sci. Eng. C* **58**, 601–609 (2015).
26. Neto, A. I. *et al.* Nanostructured polymeric coatings based on chitosan and dopamine-modified hyaluronic acid for biomedical applications. *Small* **10**, 2459–2469 (2014).
27. Ryu, J. H. *et al.* Catechol-functionalized chitosan/pluronic hydrogels for tissue adhesives and hemostatic materials. *Biomacromolecules* **12**, 2653–2659 (2011).
28. Kim, H. J. *et al.* Mussel adhesion-employed water-immiscible fluid bioadhesive for urinary fistula sealing. *Biomaterials* **72**, 104–111 (2015).

Chapter 2 - Materials and Methods

2.1 Materials

2.1.1 Chitosan

Chitosan is a linear, semi-crystalline polysaccharide composed of (1 → 4)-2-acetamido-2-deoxy-β-D-glucan (*N*-acetyl D-glucosamine) and (1 → 4)-2-amino-2-deoxy-β-D-glucan (*D*-glucosamine) units¹ - Figure 2.1. CHT is not very present in nature, but can be easily obtained by deacetylation of a natural polymer chitin. After cellulose, chitin is the second most abundant biopolymer in nature² and is typically found in invertebrates such as: the shells of crustaceans or insect cuticles, but also in some mushrooms, green algae and yeasts^{1,3}. Thus, commercially chitosan is obtained by deacetylation of chitin and has a degree of deacetylation between 66 and 95%⁴.

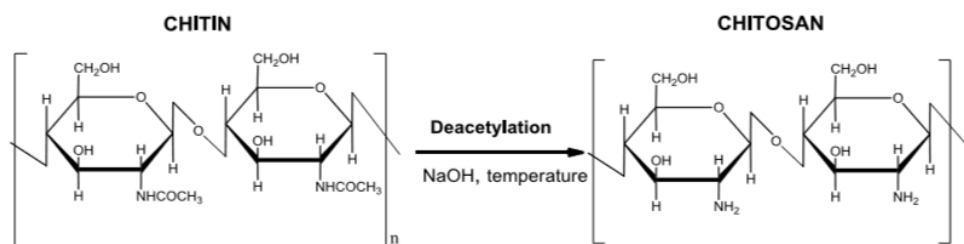


Figure 2.1 - Deacetylation of chitin. Adapted from [30].

The degree of deacetylation (DD) of chitosan, which indicates the number of amino groups along the chains, is calculated as the ratio of *D*-glucosamine with the sum of *D*-glucosamine and *N*-acetyl-*D*-glucosamine¹. The deacetylation of chitin by chemical hydrolyses is conducted under severe alkaline conditions or by enzymatic hydrolysis in the presence of specific enzymes. To obtain the product called “chitosan”, the deacetylated chitin should contain at least 60% of residues of *D*-glucosamine, which corresponds to a degree of deacetylation of 60%⁵.

Due to the presence of amino groups, chitosan is soluble in aqueous acid media and forms viscous solutions that can be used to produce gels in various ways, for example: beads, membranes, fiber, sponges and coatings. The chitosan amino group and hydroxyl ensure that it is easily chemically changed⁶. The solubility of CHT depend on the degree of deacetylation, on the protonation of free amino groups and pH. On the other hand,

swelling property of chitosan decreases with an increase in the concentration of crosslinking agent.

Chitosan is a biopolymer that exhibits great properties, as biocompatibility, biodegradability and is also non-toxic⁴. Most of these peculiar properties arise from the presence of primary amines along in its molecular structure. Due these features, this polysaccharide is a relevant material in the biomedical field, for example: in drug delivery systems, tissue engineering and ophthalmology (contact lenses)⁷. So, chitosan is no longer more a waste by product form the seafood processing industry, but a useful compound in the human health field. Chitosan was purchased from Sigma Aldrich, with an N-deacetylation degree of 81% and a molecular weight obtained by viscosimetry of 770 kDa, and purified by recrystallization.

2.1.2 Genipin

Biodegradable polymers such as chitosan often need to be crosslinked to improve their mechanical properties. Some compounds have been used for chitosan crosslinking, such as glutaraldehyde or epoxy compounds⁸. However, studies have shown that synthetic crosslinking reagents have some cytotoxicity and can damage the biocompatibility of a delivery system⁸. Thus, it is necessary to find a crosslinking reagent for biomedical applications that has low cytotoxicity and forms stable and biocompatible crosslinked products. Genipin is a natural-origin alternative crosslinking agent that fulfills these criteria⁹ - Figure 2.2. This crosslinking agent is extracted from *Gardenia jasminoides* Ellis fruits, through a modern microbiological process⁸, and has been used in traditional Chinese medicine^{10,11}. The cytotoxicity of genipin is significantly lower than some synthetic crosslinkers already mentioned. Moreover, the biocompatibility of the materials crosslinked with genipin is superior to those crosslinked with glutaraldehyde or epoxy compounds¹². This crosslinking agent has been widely used in the field of biomaterials especially in studies of tissue fixation and regeneration in biological tissues or in studies of drug delivery of macrogels and microspheres, leading to matrices with good mechanical properties and reduced swelling extent¹³.

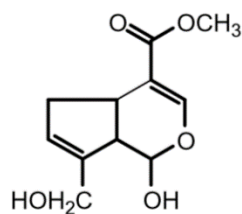


Figure 2.2 - Schematic of genipin chemical structure. Adapted from [38].

Beyond the knowledge of the use of genipin in traditional medicine, today we have some information about the beneficial effects of genipin in biochemically terms. This compound has been used for the treatment of cirrhosis of the liver, symptoms of type 2 diabetes and in addition genipin shows remarkable effects as an anti-inflammatory agent and anti-angiogenesis⁸. Genipin ($M_w = 226.23$ g/mol) was purchased from Wako chemical and used as received.

2.1.3 Dopamine

Dopamine, ordinarily known as a neurotransmitter, is a biomolecule mimic of the adhesive component DOPA of marine mussels^{14,15}. DOPA is a catecholic amino acid arising from posttranslational modification of tyrosine, and in addition to being an adhesion promoter, is also characterized as a crosslinking precursor¹⁶.

Under alkaline conditions, the catechol functional group oxidizes to quinone enabling dopamine to self-polymerize and form thin films on different surfaces through covalent and noncovalent bonds^{15,17,18}- Figure 2.3. However the exact polymerization mechanism is unknown¹⁵.

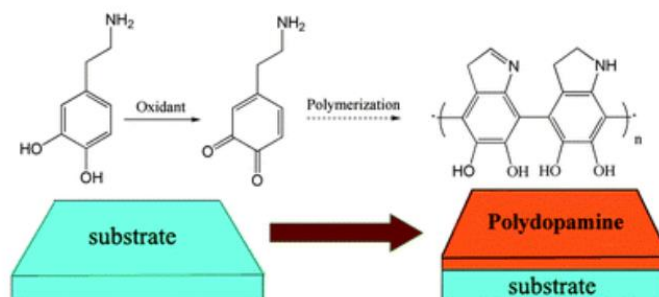


Figure 2.3 - Dopamine polymerization. Adapted from [17].

The fact that dopamine can self-polymerize and coat virtually any material and its catechol and amine functional groups can support various reactions, makes polydopamine

(PDA) an attractive multifunctional coating and bioadhesive. Thus, PDA has emerged in the recent years as a highly promising bio-inspired coating and adhesive primer¹⁹. It has been widely used to prepare a variety of ad-layers, such self-assembled monolayers through deposition of long-chain molecular building blocks, modification of inorganic surfaces, multilayer films, nanocapsules for drug delivery and bioinert and bioactive surfaces of macromolecules¹⁸. Dopamine hydrochloride ($M_w=189.64$ g/mol) was purchased of Sigma Aldrich and used without any further purification.

2.2 Methods

2.2.1 Production of chitosan films

Chitosan membranes were prepared by solvent casting, according to the procedure proposed by Caridade and co-workers¹¹. Chitosan was dissolved at 1wt.% in 1wt.% aqueous acid acetic (160mL). Then, 10mL of a 1.8×10^{-2} M genipin solution was added dropwise to the chitosan solution under stirring. Non-crosslinked chitosan membranes were prepared directly from the original solutions, without adding genipin solution. The solutions were cast in Petri dishes and, approximately 12 hours later, a blue color typical of the crosslinking reaction with genipin appeared. The solutions with genipin were properly protected from light. The mechanism proposed by Mi *et al*²⁰ of the crosslinking reaction chitosan with genipin is depicted in figure 2.4, in which a crosslinked chitosan network is established.

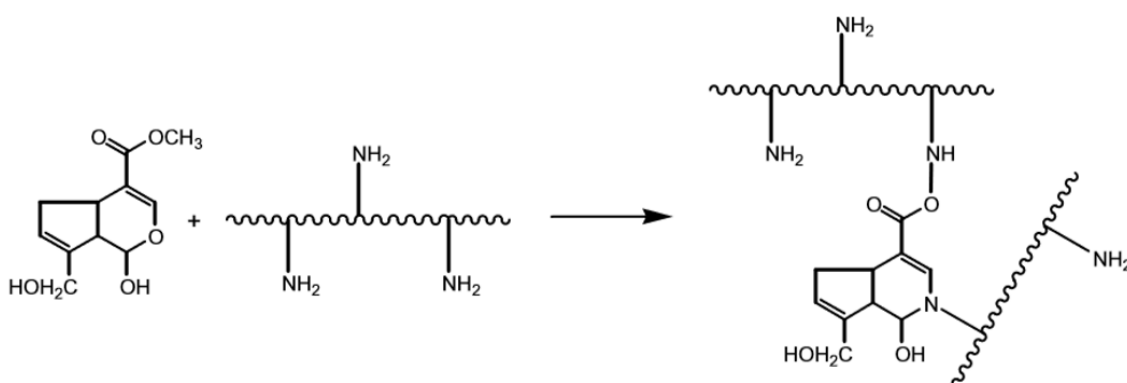


Figure 2.4 - Schematic representation of the crosslinking reaction chitosan with genipin. Adapted from [20].

The crosslinking degree (x) was defined as the reagents feed molar ratio considering the stoichiometry of the expected crosslinking reaction:

$$X (\%) = \frac{2n_{GP}}{n_{NH_2}} \times 100$$

Where n_{GP} and n_{NH_2} are the molar amounts of genipin and chitosan amino groups. From this definition, the crosslinking degree was calculated to be 0.1%, 1% and 2%. After drying the solutions at room temperature, both crosslinked and non-crosslinked chitosan membranes were peeled off and neutralized in a 0.1M NaOH solution for about 10 minutes. After, they were washed thoroughly with distilled water until the pH was equal to 7, and they were dried again - Figure 2.5.

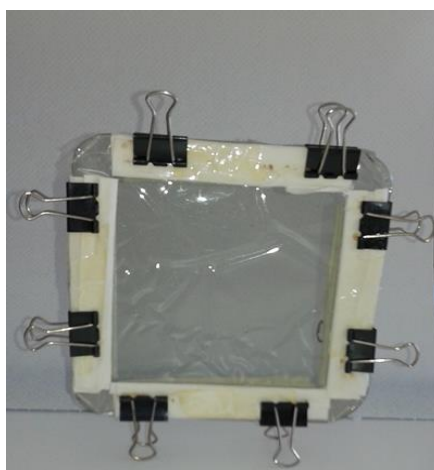


Figure 2.5 - Drying process of a chitosan film.

2.2.2 Coating of the films with polydopamine

The polydopamine coating was performed according the procedure of Lee and co-workers¹⁵. The membranes were dipped in 2mg/mL dopamine solution in 10mM Tris, pH= 8.5, for 24hours, at room temperature. Besides, the dopamine concentration of 2mg/mL, two other concentrations were also tested, 0.5 mg/mL and 1mg/mL in order to verify how the concentration of dopamine affects the coating process. It was also tested a deposition time of 48 hours and a temperature of 37°C.

A 10mM Tris buffer solution was prepared and adjusted at pH= 8.5 (which is the typical pH of marine environment). Posteriorly, dopamine was dissolved in Tris solution previously prepared. Dopamine is very sensitive to air and to light, so the containers were lined with aluminum foil. Finally the membranes were covered with dopamine solution, as shown in the figure 2.6, and stored at room temperature. The membranes treated at 37

degrees were stored in an oven. Different samples were immersed at both 24 hours and 48 hours, for each temperature.

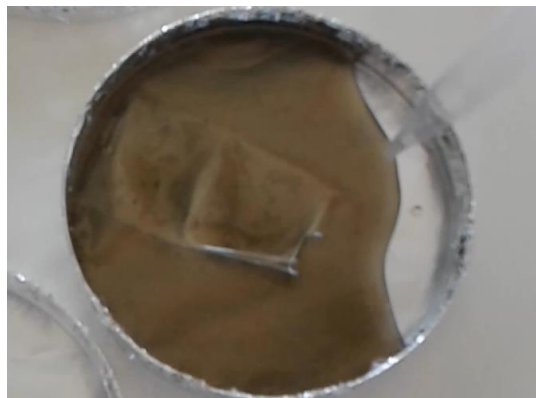


Figure 2.6 - Dopamine coating films.

When the chosen deposition time finished, all the samples were properly washed with distilled water and dried.

Based on a previous work, the coating of chitosan membranes was made following the experimental conditions described by Lee and co-workers¹⁵, 2 mg/mL dopamine solution in 10mM Tris, pH=8.5 for 24h at room temperature.

2.2.3 Characterization techniques

Several characterization techniques, namely UV-Vis spectroscopy, FTIR, H-NMR, SEM, AFM and contact angles measurements were used in this work to analyze if the coating procedure was successful and also to characterize the properties of the coated membranes. In next sub-section, a short description of these techniques will be given.

2.2.3.1 Fourier Transform Infrared Spectroscopy (FTIR)

Infrared radiation (IR) of frequencies less than about 100 cm^{-1} is absorbed and converted by an organic molecule into energy of molecular rotation. This absorption is quantized and the molecular rotation spectrum consists of discrete lines. IR in the range from about $10000\text{-}100\text{ cm}^{-1}$ is absorbed and converted by an organic molecule into energy of molecular vibration²¹. This absorption is also quantized but vibrational spectra appear as bands rather than as lines because a single vibrational energy change is accompanied by a number of rotational energy changes. Thus, FTIR spectroscopy is based on the vibrational excitation of molecular bonds by absorption of IR light energy and the sum of vibrational spectra for a compound can produce an infrared absorption spectrum that looks like its molecular “fingerprint”²². The wavelength of absorption depends on the

relative masses of the atoms, the force constants of the bonds and the geometry of the atoms.

Band position in IR spectra are presented here as wavenumbers ($\bar{\nu}$) whose unit is the reciprocal centimetre (cm^{-1}), this unit is proportional to the energy of vibration. On the other hand band intensities can be expressed either as transmittance (T) or absorbance (A). Transmittance is the ratio of the radiant power transmitted by a sample to the radiant power incident on the sample. Absorbance is the logarithm, to the base 10, of the reciprocal of the transmittance²¹:

$$A = \log_{10} \left(\frac{1}{T} \right)$$

Spectra ranging between 4000 and 400 cm^{-1} were performed with an ATR-FTIR JASCO equipment, with a support coupled to films analysis. It was not possible to confirm the presence of polydopamine with the results of this technique, so the FTIR spectra will be present only in annex and not in Chapter 3.

2.2.3.2 Ultraviolet spectrometry (UV-Vis)

Molecular absorption in the ultraviolet (UV) and visible region of the spectrum is dependent on the electronic structure of the molecule. Absorption of energy is quantized, resulting in the elevation of electrons from orbitals in the ground state to higher energy orbitals in an excited state²³. With UV spectrometry characteristic groups may be recognized in molecules of widely varying complexities.

In the UV spectra, the principal characteristics of an absorption band are its position and intensity. The position of absorption corresponds to the wavelength of radiation whose energy is equal to that required for an electronic transition. The intensity of absorption may be expressed as transmittance (T) defined by²⁴:

$$T = \frac{I}{I_0}$$

Where I_0 is the intensity of the radiation energy striking the sample, and I is the intensity of the radiation emerging from the sample. A more convenient expression of absorption intensity is that derived from Lamber-Beer law:

$$A = \log_{10} \frac{I_0}{I} = kcb$$

Where A is Absorbance, k a constant characteristic of the solute, c concentration of solute (moles per millimetre) and b path length through the sample (centimetres). The preceding expression becomes:

$$A = ec b$$

The term e is known as the molar absorptivity, formerly called the molar extinction coefficient. The intensity of an absorption band in the UV spectrum is usually expressed as the molar absorptivity at maximum absorption²⁴.

The instrument must allow an appropriate wavelength to be selected suitable for the particular analyte. The sample and reference must be placed in the light beam in such a way that the ratio of the transmitted radiation beams can be measured. Finally, the transmittance value or preferably the absorbance value should be displayed and recorded²⁵. Tests were performed in a Shimadzu equipment in a range of 800 and 250 nm, with a support coupled to films analysis.

2.2.3.3 Proton Nuclear Magnetic Resonance (H-NMR)

Nuclear magnetic resonance spectrometry basically is another form of absorption spectrometry, similar to IR or UV spectrometry. However with knowledge of basic theory, interpretation of NMR spectra is usually feasible in greater detail than is the case of IR or UV spectra.

All nuclei carry a charge, and in some nuclei this charge spins on the nuclear axis and this circulation of nuclear charge generates a magnetic dipole along the axis. The angular momentum of the spinning charge can be described in terms of spin numbers I , these numbers have values of $0, \frac{1}{2}, 1, \frac{3}{2}$ and so on²⁶. The intrinsic magnitude of the generated dipole is expressed in terms of nuclear magnetic moment, μ .

The nuclear magnetic moment, μ , is directly proportionally to the spin²⁷:

$$\gamma = \frac{2\pi\mu}{hI}$$

Where the proportionally constant, is called the magnetogyric ratio and is a constant for each particular nucleus, and h is Planck's constant.

In quantum mechanical terms the spin number I determines the number of orientations a nucleus may assume in an external uniform magnetic field. The fundamental NMR equation correlating electromagnetic frequency with magnetic field strength:

$$\nu = \frac{\gamma B_0}{2\pi}$$

Where ν is the frequency of electromagnetic radiation, γ the magnetogyric ratio and B_0 the magnetic field.

The peak area (measured by an electronic integrator) is proportional to the number of protons it represent, and the peak positions are measured in frequency units from a reference peak. A proton count from the integration is useful to determine or confirm molecular formulas, detect hidden peaks, determine sample purity and do quantitative analysis. The ideal solvent should contain no protons and be inert, nonpolar, low-boiling and inexpensive²⁷.

5mg of the membranes were cut and added to 0,96mL of deuterated water (D₂O) and 0.04 mL of deuterated hydrochloric acid (DCL). To promote the dissolution, the solution was heated in a water bath at 70°C for 48hours. The NMR analyses were performed in a Varian Unity Plus 300 equipment, at 70° C. Unfortunately, crosslinking and coated chitosan membranes did not dissolved in these conditions. So it was possible to analyze only the spectrum of pure chitosan, and from this spectrum it was calculated the degree of deacetylation.

2.2.3.4 Scanning Electron Microscopy (SEM)

Image formation in SEM depends on the acquisition of signals produced from the electron beam and specimen interactions. From the interaction between the electronic beam and the sample results the emission of various types of radiation and electrons, such as: secondary electrons, X-ray, Auger electrons, photons, etc^{28,29}. These radiations, when properly captured, will provide information of sample characteristics, such as composition, surface topography or crystallography.

The most widely signal used in formulation of images is the signal of secondary electrons^{29,30}. Secondary electrons are low-energy electrons that are emitted when the primary electron beam strikes the samples surface, that is, they are electrons from the sample where occurs excitation and “escape” from the surface. They provide the sample surface topography and they are the responsible for obtaining the high-resolution images.

The samples must satisfy the following characteristics to be characterized by SEM: (1) present good surface conductivity- the absence of conductivity leads to the need of metallization, by applying un ultra-thin coating of Au or C, (2) Support vacuum conditions,(once the SEM uses an electron beam which makes necessary the uses of vacuum) and(3) physical and chemical stability. Scanning electron microscopy (SEM) is

used for the analysis and examination of the microstructure morphology and chemical characterization of surfaces. The morphology of all the produced membranes were characterized by using a JSM-6010LV SEM (JEOL, Japan). The experiments were performed using the secondary electron imaging (SEI) mode with accelerating voltage of 10Kv previously gold coated samples.

2.2.3.5 Atomic force microscopy (AFM) coupled with nanoindentation tests

The atomic force microscope is an instrument based on detection of the interaction force between a microscopic tip and a sample surface (Figure 2.7), and it allows to obtain 3D images at expansions of the order magnitude of 10^9 times the surface of the samples. Normally, the AFM technique was coupled with nanoindentation tests, in order to provide the combination of topographic images with nanomechanical properties of the samples³¹. Nanoindentation studies of the adhesion refer to values of the adhesion force, which is measured as the external pulling force required to detach the indenter from the sample³².

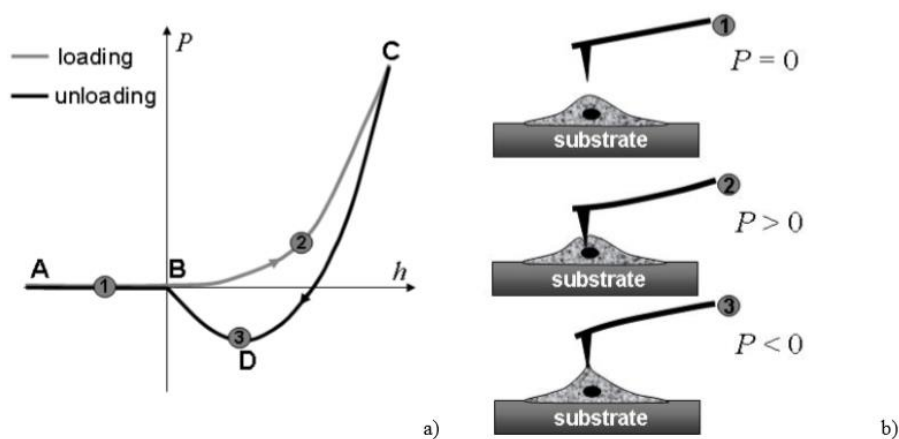


Figure 2.7 - a) Scheme of a typical force versus the AFM tip displacement acquired in indentation of a surface. b) States of the AFM probe corresponding to the three points figured on the force curve. Adapted from [56]

Figure 2.7 a) shows schematically a typical force curve obtained in a surface indentation affected by adhesion. In the beginning of the teste when the AFM tip is far from the cell surface, the interaction force is zero (position 1). Then, the AFM tip is impinging on the membrane with a positive indentation force (position 2). After loading, the AFM probe is retracted and the impinging force is decreasing, the interaction becomes

negative (position 3) and the tip is pulling up the surface. The indentation is affected by the adhesion force between the AFM tip and surface membrane. The AFM analysis were used to assess the topography, the mechanical and adhesion properties of the membranes. All membranes were imaged using a Dimension Icon AFM equipment (Bruker, France) with a spring constant of 0.12 N/m and a silicon tip on nitride lever at a frequency of 23 kHz, operating in a ScanAsyst mode.

2.2.3.6 Water Contact angle measurement

The contact angle is defined as the angle formed by the intersection of the liquid-solid interface and the liquid-vapor interface³³. This angle is acquired applying a tangent line from de contact area along the vapor interface in the droplet profile - Figure 2.8.

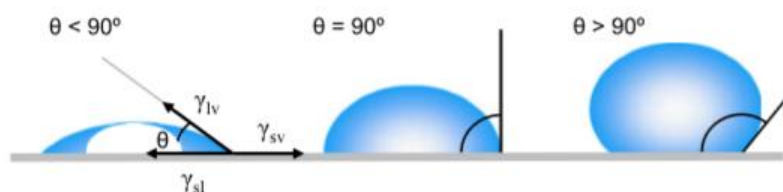


Figure 2.8- General illustration of contact angle formed by sessile liquid drops. Adapted from [58]

The contact angle of a water drop (on an ideal surface) is defined by the equilibrium of the drop under the action of the three interfacial tensions described in figure 2.8. The balance between these forces is described by Young's equations³⁴:

$$\gamma_{SV} - \gamma_{SL} = \gamma_{LV} \cos \theta$$

Where γ_{SV} is the solid surface free energy, γ_{SL} is the solid-liquid interfacial free energy γ_{LV} is the liquid surface free energy (also called surface tension) and θ is the contact angle. The angle expresses the hydrophobic or hydrophilic character of the surface according to its value - Table 2.1:

Table 2.1- Hydrophilic and hydrophobic character depending on the contact angle value. Adapted from [60].

$\Theta = 0$	Highly hydrophilic
$\Theta < 90^\circ$	Hydrophilic surface
$\Theta \geq 90^\circ$	Hydrophobic surface
$\Theta > 160^\circ$	Super-hydrophobic

That means, in other words, that contact angles greater than 90° indicates that wetting of the surface is unfavourable, so the fluid will minimize its contact with the surface and form a compact liquid droplet (hydrophobic surface). While contact angles less than 90° means that wetting surface is favourable and the fluid will spread over a large area on the surface (hydrophilic surface)³⁵. Static contact angle measurements were carried out by the sessile drop method using a contact angle meter (model OCA 15+) with a high-performance image processing system from DataPhysics Instruments (Filderstadt, Germany). A drop (5 µ L) of water was added by a motor driven syringe at room temperature. The results treatment were performed with the SCA20 *software* and at least three measurements of each condition were performed on each membrane surface.

2.2.3.7 Bioadhesion tests

Lap-shear stress adhesion tests of the coated and uncoated CHT membranes were performed, following the experimental set-up illustrated in Figure 2.9. These tests involved mounting of samples in a electromechanical testing machine, and they were submitted to a controlled tensile force until the detachment of the CHT membranes from the pigskin.

Stress-strain experimental curves were obtained, through which was possible to determine the maximum stress involved in the sample detachment, the bioadhesive strength obtained in this work.

The pig skin used to perform these bioadhesion tests was extracted from the pig ear and it was previously cleaned from the fat layer, hair and other impurities. Then, the CHT membranes and the pig skin were cut with the same dimensions following the ASTM D 1002, 10mm length and 5mm width. Then, these membranes were superimposed on the pig skin and kept under load in a PBS (0,01M) for 48 hours. The chitosan membranes and the pigskin were always kept in PBS solution, to keep them hydrated.

Finally, lap-shear adhesive tests were performed in a Zwick Roell Z005 equipment, with a charge of 5kN. The experiments were performed with a velocity of 0.3 mm/min.

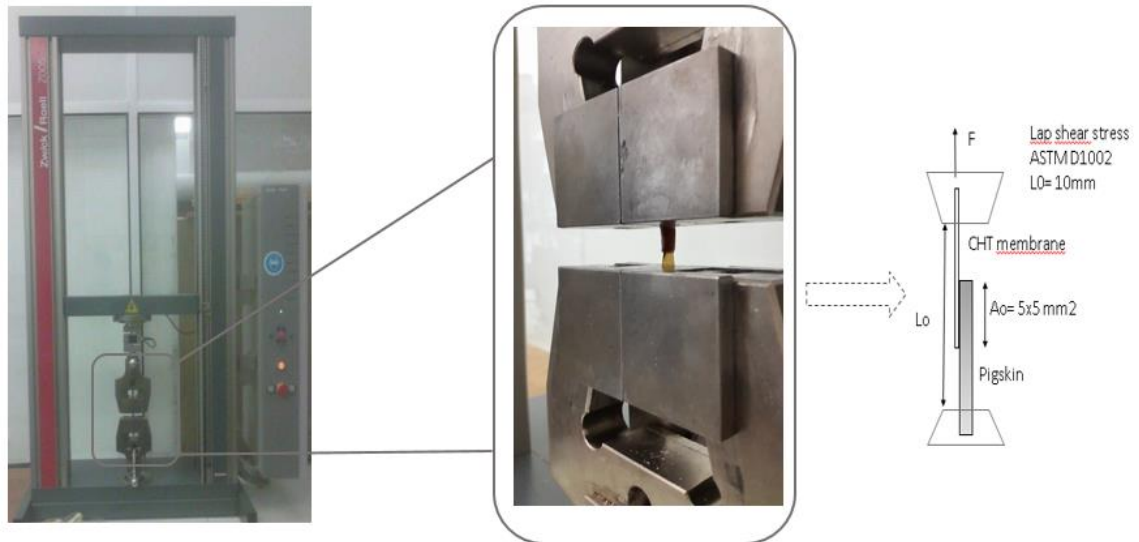


Figure 2.9- Equipment used to performed adhesion tests and their schematic illustration. Where L_0 is the gauge length and A_0 is the overlapping area.

References

1. Croisier, F. & Jérôme, C. Chitosan-based biomaterials for tissue engineering. *Eur. Polym. J.* **49**, 780–792 (2013).
2. Rinaudo, M. Chitin and chitosan: Properties and applications. *Prog. Polym. Sci.* **31**, 603–632 (2006).
3. Ravi Kumar, M. N. . A review of chitin and chitosan applications. *React. Funct. Polym.* **46**, 1–27 (2000).
4. Bansal, V., Sharma, P. K., Sharma, N., Pal, O. P. & Malviya, R. Applications of Chitosan and Chitosan Derivatives in Drug Delivery. *Biol. Res.* **5**, 28–37 (2011).
5. Van De Velde, K. & Kiekens, P. Structure analysis and degree of substitution of chitin, chitosan and dibutylchitin by FT-IR spectroscopy and solid state¹³C NMR. *Carbohydr. Polym.* **58**, 409–416 (2004).
6. Jin, J., Song, M. & Hourston, D. J. Novel chitosan-based films cross-linked by genipin with improved physical properties. *Biomacromolecules* **5**, 162–168 (2004).
7. Dutta, P. K., Duta, J. & Tripathi, V. S. Chitin and Chitosan: Chemistry, properties and applications. *J. Sci. Ind. Res. (India)*. **63**, 20–31 (2004).
8. Muzzarelli, R. A. A. Genipin-crosslinked chitosan hydrogels as biomedical and pharmaceutical aids. *Carbohydrate Polymers* **77**, 1–9 Genipin, a crystalline and well defined chemical (2009).
9. Butler, M. F., Ng, Y. F. & Pudney, P. D. A. Mechanism and kinetics of the crosslinking reaction between biopolymers containing primary amine groups and genipin. *J. Polym. Sci. Part A Polym. Chem.* **41**, 3941–3953 (2003).
10. Artech Pujana, M., Pérez-Álvarez, L., Cesteros Iturbe, L. C. & Katime, I. Biodegradable chitosan nanogels crosslinked with genipin. *Carbohydr. Polym.* **94**, 836–842 (2013).
11. Caridade, S. G., da Silva, R. M. P., Reis, R. L. & Mano, J. F. Effect of solvent-dependent viscoelastic properties of chitosan membranes on the permeation of 2-phenylethanol. *Carbohydr. Polym.* **75**, 651–659 (2009).
12. Chen, M. C. *et al.* Mechanical properties, drug eluting characteristics and in vivo performance of a genipin-crosslinked chitosan polymeric stent. *Biomaterials* **30**, 5560–5571 (2009).
13. Silva, S. S. *et al.* Genipin-modified silk-fibroin nanometric nets. *Macromol. Biosci.* **8**, 766–774 (2008).

14. Lee, H., Rho, J. & Messersmith, P. B. Facile conjugation of biomolecules onto surfaces via mussel adhesive protein inspired coatings. *Adv. Mater.* **21**, 431–434 (2009).
15. Lee, H., Dellatore, S. M., Miller, W. M. & Messersmith, P. B. Mussel-inspired surface chemistry for multifunctional coatings. *Science* **318**, 426–430 (2007).
16. Murphy, J. L., Vollenweider, L., Xu, F. & Lee, B. P. Adhesive performance of biomimetic adhesive-coated biologic scaffolds. *Biomacromolecules* **11**, 2976–2984 (2010).
17. Lee, H., Scherer, N. F. & Messersmith, P. B. Single-molecule mechanics of mussel adhesion. *Proc. Natl. Acad. Sci. U. S. A.* **103**, 12999–13003 (2006).
18. Wei, Q., Zhang, F., Li, J., Li, B. & Zhao, C. Oxidant-induced dopamine polymerization for multifunctional coatings. *Polym. Chem.* **1**, 1430 (2010).
19. Guardingo, M. *et al.* Bioinspired Catechol-Terminated Self-Assembled Monolayers with Enhanced Adhesion Properties. *Small* **10**, 1594–1602 (2013).
20. Mi, F. L., Sung, H. W. & Shyu, S. S. Synthesis and characterization of a novel chitosan-based network prepared using naturally occurring crosslinker. *J. Polym. Sci. Part A Polym. Chem.* **38**, 2804–2814 (2000).
21. Silverstein, Bassler, M. *Spectrometric identification of organic compounds.* (1996).
22. Taha, M., Hassan, M., Essa, S. & Tartor, Y. Use of Fourier transform infrared spectroscopy (FTIR) spectroscopy for rapid and accurate identification of yeasts isolated from human and animals. *Int. J. Vet. Sci. Med.* **1**, 15–20 (2013).
23. Schmid, F. Biological Macromolecules : UV-visible Spectrophotometry. *Encycl. Life Sci.* 1–4 (2001).
24. Silverstein, Bassler, M. *Spectrometric identification of organic compounds.* (1995).
25. C. Denney, Ronald, R. S. *Visible and ultraviolet spectroscopy.* (1996).
26. Victor A. Gault, N. H. M. *Understanding Bioanalytical Chemistry: Principles and Applications.* (2009).
27. R.J Abraham, J.Fisher, P. L. *Introduction to NMR Spectroscopy.* (1995).
28. Vernon-Parry, K. D. Scanning electron microscopy: an introduction. *III-Vs Rev.* **13**, 40–44 (2000).
29. Fonseca, A. M. *Análises de materiais e superfícies.* 5–20 (2013).

30. Denk, W. & Horstmann, H. Serial Block-Face Scanning Electron Microscopy to Reconstruct Three-Dimensional Tissue Nanostructure. *PLoS Biol.* **2**, e329 (2004).
31. Sirghi, L. Atomic Force Microscopy indentation of living cells. *Microsc. Sci. Technol. Appl. Educ.* **4**, 433–440 (2010).
32. Sirghi, L. & Rossi, F. The effect of adhesion on the contact radius in atomic force microscopy indentation. *Nanotechnology* **20**, 365702 (2009).
33. Yuan, Y. & Lee, T. R. *Surface Science Techniques.* **51**, (2013).
34. Lamour, G. *et al.* Contact angle measurements using a simplified experimental setup. *J. Chem. Educ.* **87**, 1403–1407 (2010).
35. Assis, O. B. G. Alteração do caráter hidrofílico de filmes de quitosana por tratamento de plasma de HMDS. *Quim. Nov.* **33**, 603–606 (2010).
36. Davis, J. R. Introduction to Tensile Testing. *Tensile Test.* 1–13 (2004).
37. Gedney, R. Guide to Testing Metals Under Tension. *Adv. Mater. Process.* 29–31 (2002).

Chapter 3 - Modification of chitosan based membranes with polydopamine

Abstract

In marine environment, mussels are able to secrete specific proteins that act as a glue, allowing them to strongly attach to distinct substrates. The outstanding adhesive properties of mussels have been attributed to the presence of the catechol groups in such proteins, which are also present in the small molecule dopamine.

Inspired by the structure of the adhesive proteins in mussels and by the properties of the natural polysaccharide chitosan, herein we report the production of chitosan membranes both uncrosslinked and crosslinked with genipin that were modified with a polydopamine coating. The unmodified crosslinked and uncrosslinked chitosan membranes were used as controls. The membranes were characterized by ultraviolet-visible spectrophotometry, scanning electron microscopy, atomic force microscopy and water contact angle measurements. Finally, bioadhesion tests were performed on pig skin. The results confirmed the presence of polydopamine on the modified membranes, where polydopamine formed a self-polymerized coating on both uncrosslinked and crosslinked membranes. It was shown that the unmodified crosslinked and uncrosslinked membranes possessed a rougher surface than the modified membranes. The presence of polydopamine on the modified membranes, both uncrosslinked and crosslinked, led to smoother surfaces and increased their hydrophilicity. Both AFM coupled with nanoindentation tests and bioadhesion tests confirmed that the polydopamine coating improved the adhesive properties of both uncrosslinked and crosslinked modified membranes. The developed membranes could be potentially used in skin wound healing.

Keywords: Marine mussels, polydopamine, chitosan, coating

3.1 Introduction

Nature abounds examples of functional materials. There has been a great interest by the scientific community to mimic Nature in order to generate high-performing and environmentally friendly materials. Among them, mussel adhesive proteins (MAPs) are

one of the most interesting and studied examples once they are water-resistant being able to adhere on wet surfaces^{1,2}.

One unique structural feature of MAPs is the presence of 3, 4 dihydroxyphenylalanine (DOPA), a catecholic amino acid arising from posttranslational modification of tyrosine³⁻⁵. Catechol groups were identified by Wait and Tazer⁶, in 1981, and they are responsible for the versatile adhesion of mussels in adverse environmental conditions. Mussels can attach to different types of surfaces in aqueous conditions, such natural inorganic materials (e.g., rocks), organic materials (e.g., fish skins) and synthetic materials (e.g., Teflon)⁷. Based on these findings, fascinating advancements were done in order to mimic the chemical composition of MAPS and their adhesive properties^{3,8}. Dopamine is a well known neurotransmitter catecholamine present in a variety of animals. It has been found that, under alkaline conditions, the catechol functional groups oxidize allowing dopamine to self-polymerize and form an adhesive polydopamine (PDA) layer on a variety of material surface through covalent and noncovalent bonds^{2,9-13}. Namely, it has been shown that a polydopamine coating is able to form on: noble metals, metals with native oxide surfaces (Cu and stainless steel), oxides [TiO₂ and Crystalline SiO₂ (quartz)], semiconductors, ceramics (glass and hydroxyapatite) and synthetic polymers⁸. The coating of a variety of substrates with polydopamine has been investigated by several authors^{10,12,14-16}. For example, Tsai *et al*¹⁷ have coated several biodegradable polymers such as polycaprolactone, poly (L-lactide), poly (lacti-co- glycolic acid) and polyurethane with PDA. They used evaluated the attachment and proliferation of rabbits chondrocytes for potential application in articular cartilage tissue engineering. It was shown that chondrocytes adhesion and proliferation on the studied biodegradable polymers was significantly increased by soaking them in an alkaline dopamine solution for only a few minutes¹⁷. Yang *et al*¹⁸, proposed a new approach for the individual encapsulation of yeast living cells, by coating them with a functionalizable PDA layer. They concluded that polydopamine encapsulation is a versatile and simple method to introduce various functionalities onto the cell surface under physiologically compatible conditions. Messersmith *et al*¹⁹ tried to mimic the adhesion features demonstrated by the foot of the gecko. They produced a hybrid biological adhesive which contained an array of nanofabricated polymer pillars coated with a layer of another polymer containing dopamine units. They found that the adhesion of the polymer pillars increased nearly 15-fold after coating them with the dopamine unit containing polymer.

. The aim of the present work was to produce and evaluate the properties of natural membranes made of chitosan (CHT) and CHT membranes crosslinked with genipin submitted to a PDA coating. The produced membranes were characterized by ultraviolet-visible spectrophotometry, scanning electron microscopy, atomic force microscopy, contact angle measurements and adhesion tests.

CHT is the N-deacetylation product of chitin. Chitin is a polysaccharide commonly found in the exoskeleton of crustaceans and insects²⁰, but also in some mushrooms envelopes, green algae cell walls and yeasts²¹, and is the second most important natural polymer in the world.²²⁻²⁴ In terms of applications, CHT is the most important chitin derivate²². CHT is a linear, semi-crystalline polysaccharide composed of (1 → 4)-2-acetamido-2-deoxy-β-D-glucan (*N*-acetyl D-glucosamine) and (1 → 4)-2-amino-2-deoxy-β-D-glucan (D-glucosamine) units²¹. This biopolymer exhibits great properties, as a biocompatibility, biodegradability and non-toxicity. Because of these features this polysaccharide is a relevant candidate in the field of biomaterials, especially for tissue engineering.

As other biodegradable polymers, CHT is often crosslinked to model and improve their properties. In this work, CHT membranes are crosslinked with genipin in order to verify if the presence of this crosslinking favors the PDA coating as its adhesive properties. Genipin is a natural crosslinking agent, extracted from gardenia fruits and it is found in the traditional Chinese medicine²⁵⁻²⁸. Genipin has been widely employed in studies of tissue fixation, regeneration in various biomaterials and natural biological tissues or in drug delivery studies²⁹.

Attending to the features of these three materials, which are already widely studied and used in the biomedical field, we believe that the membranes developed in this work could have a great potential to be used in tissue engineering, namely to treat and recover damaged skin. Herein, it is expected that the produced membranes possessing the PDA coating will present bioadhesive properties that will allow their attachment to skin. Bioadhesion is defined as a phenomenon occurring at the interface between a natural or synthetic macromolecule and a biological substrate³⁰. Bioadhesives play essential roles in many living systems and are considered to be very promising biomaterials for use in biotechnology and tissue engineering due of their versatile adhesion properties, biocompatibility and biodegradability³¹.

3.2 Experimental

3.2.1 Materials

Chitosan (CHT) (medium molecular weight) was purchased from Sigma-Aldrich (Germany) and purified by a reprecipitation method prior to use. The degree of *N*-deacetylation (DD) was found to be 81 % by H-NMR, according to the procedure described by V.Sencadas³² and the molecular weight (M_v) was determined by viscosimetry in CH_3COOH 0.5 M/ NaCH_3COO 0.2 M, which was found to be 770 kDa according to the Mark-Houwink theory ($k = 3.5 \times 10^{-4}$; $a = 0.76$)³³.

Genipin (GP, $M_w = 226.23$ g/mol) was purchased from Wako chemical (USA) and used as received. Dopamine hydrochloride ($M_w = 189.64$ g/mol) was purchased of Sigma Aldrich and used without any further purification. Tris-HCl ($M_w = 157.56$) and all other reagents and solvents used were of reagent grade and were used without further purification.

3.2.2 Production of chitosan membranes

CHT membranes were prepared by solvent casting, according to the procedure proposed by Caridade and co-workers.²⁷ CHT was dissolved at 1wt. % in 1wt. % aqueous acid acetic (160mL). Then, 10mL of a 1.8×10^{-2} M genipin solution was added dropwise to the CHT solution under stirring. Non-crosslinked CHT membranes were prepared directly from the original solutions, without adding genipin solution. The solutions were cast in Petri dishes and, approximately 12 h later, a blue color typical of the crosslinking reaction with genipin appeared. The crosslinking degree (x) was defined as the reagents feed molar ratio considering the stoichiometry of the expected crosslinking reaction:

$$X (\%) = \frac{2n_{GP}}{n_{NH_2}} \times 100$$

Where n_{GP} and n_{NH_2} are the molar amounts of GP and CHT amino groups. From this definition, the crosslinking degree was calculated to be 0.1%, 1% and 2%. After the evaporation of the solutions at room temperature, both crosslinked and non-crosslinked chitosan membranes were peeled off and neutralized in a 0.1M NaOH solution for about 10 minutes, and washed thoroughly with distilled water and dried again.

3.2.3 Polydopamine coatings on the uncrosslinked and crosslinked membranes

The polydopamine coating was performed according to the procedure of Lee and co-workers¹⁶. CHT and CHT crosslinked membranes were covered with 2mg/mL dopamine solution in of 10 mM Tris, pH = 8.5 (typical pH of marine environment). The films were kept immersed in this solution for 24 hours, at room temperature, properly protected from light. Then, the membranes were thoroughly washed with distilled water and dried again.

3.2.4 Characterization of the produced membranes

3.2.4.1 UV-Visible spectroscopy (UV-Vis) measurements

All membranes were characterized by UV-Visible spectroscopy (ShimadzuUV-2501) performed in a range between 800 and 250 nm using a solid film support.

3.2.4.2 Scanning Electron Microscopy (SEM) and Atomic force microscopy (AFM)

The morphology of all the produced membranes were characterized by using a JSM-6010LV SEM (JEOL, Japan). The experiments were performed using the secondary electron imaging (SEI) mode with accelerating voltage of 10Kv previously gold coated samples.

The AFM analysis were used to assess the topography, the mechanical and adhesion properties of the membranes. All membranes were imaged using a Dimension Icon AFM equipment (Bruker, France) with a spring constant of 0.12 N/m and a silicon tip on nitride lever at a frequency of 23 kHz, operating in a ScanAsyst mode.

3.2.4.3 Water contact angle measurements (WCA)

The wettability of all surfaces was evaluated by WCA measurements. Static contact angle measurements were carried out by the sessile drop method using a contact angle meter (model OCA 15+) with a high-performance image processing system from DataPhysics Instruments (Filderstadt, Germany). A drop (5 μ L) of water was added by a

motor driven syringe at room temperature. The results treatment were performed with the SCA20 *software* and at least three measurements of each condition were performed on each membrane surface.

3.2.4.4 Bioadhesion tests

For the adhesion tests, pig skin was chosen in order to evaluate if the membranes were able to attach to it. Both membranes and pig skin were cut in large rectangular strips with 10 mm length and 5 mm width. Then, a strip of membrane and a strip of pig skin were put in contact with an overlap of $5 \times 5 \text{ mm}^2$. The assembly was dipped into a PBS solution and placed between two glass slides during 48 hours. After that, the samples were removed from the glass slides and were placed in the universal testing machine. Tensile tests were performed according to ASTM D1002 in a Zwick Roell Z005 equipment with a cell load of 5 kN under a loading speed of 0.3 mm/min and a gauge length of 10 mm.

3.3 Results and Discussion

After polydopamine coating on the uncrosslinked and crosslinked membranes, it was verified by naked eye a change of color (Figure 3.1) in all modified membranes, suggesting the presence of the PDA layer.

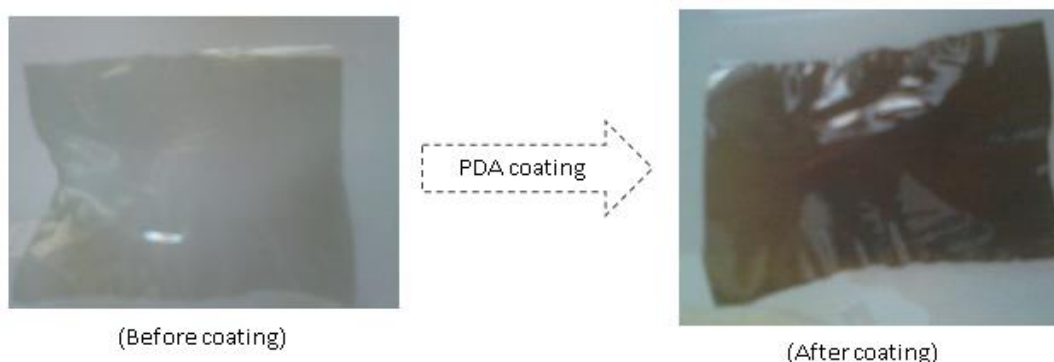


Figure 3.1 - Image of a membrane before and after coating.

3.3.1 UV-Visible spectroscopy (UV-Vis)

Figure 3.2 presents the UV-Vis spectra of the CHT and crosslinked CHT membranes at different crosslinking degrees. As the crosslinking degree of the CHT

membranes increases, a peak at 600 nm corresponding to a blue pigment, was observed and increased as the crosslinking degree of the membranes increased. Moreover, for the CHT membranes crosslinked at 0.1 % GP the peak at 600 nm is almost inexistent due the lower degree of crosslink. Pujana *et al* reported the appearance of a peak at ~600 nm that was ascribed to the crosslinking reaction between CHT and GP where its intensity was increased throughout the course of the reaction²⁹.

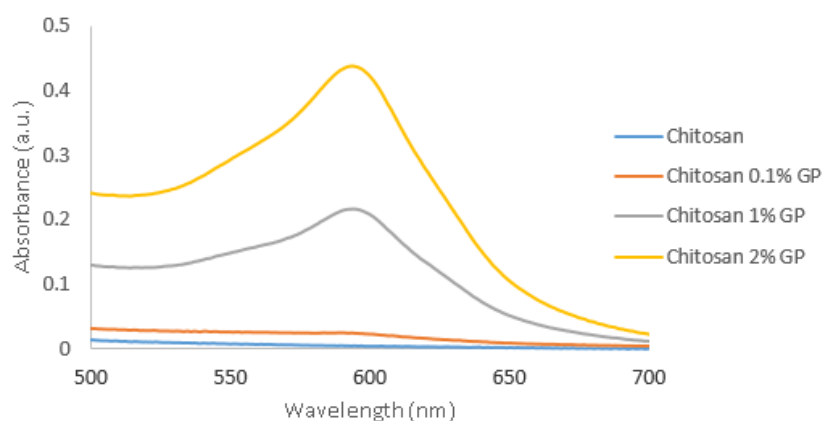


Figure 3.2- UV-Vis spectra of the CHT (blue) and crosslinked CHT membranes at different crosslinking degrees: 0.1 % (orange); 1 % (grey); and 2 % (yellow) of GP.

UV-Vis was used to detect the presence of PDA on the produced CHT and crosslinked CHT membranes with GP. Figure 3.3 shows the UV-Vis spectra of the unmodified membranes and the ones modified with PDA. A notorious increase of the absorption peak located at 290 nm was verified for the 1% and 2% GP crosslinked membranes. This increase was attributed to the formation of the heterocyclic GP-CHT compound³⁴ that was formed by a nucleophilic attack on GP by a primary amino group of CHT³⁵. For the membranes modified with PDA a broad band between 250 and 400 nm appeared confirming its presence, which is in accordance with literature^{9,36}.

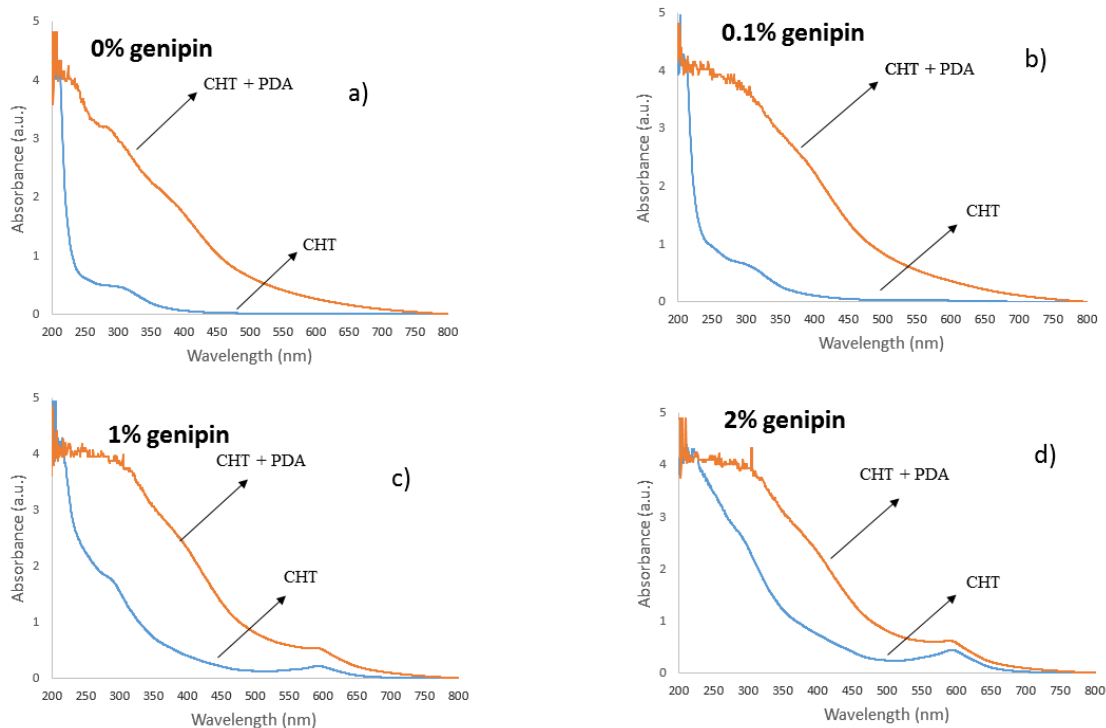


Figure 3.3- UV-Vis spectra of a) non-crosslinked CHT and non-crosslinked CHT modified with PDA membrane; b) 0.1 % crosslinked CHT and 0.1 % crosslinked CHT modified with PDA membrane; c) 1% crosslinked CHT and 1 % crosslinked CHT modified with PDA membrane and d) 2% crosslinked CHT and 2% crosslinked modified with PDA membrane.

From the results obtained, it can also be concluded that for the PDA coated membranes, the increase of GP leads to higher absorbance in the spectra. (Figure 3.4).

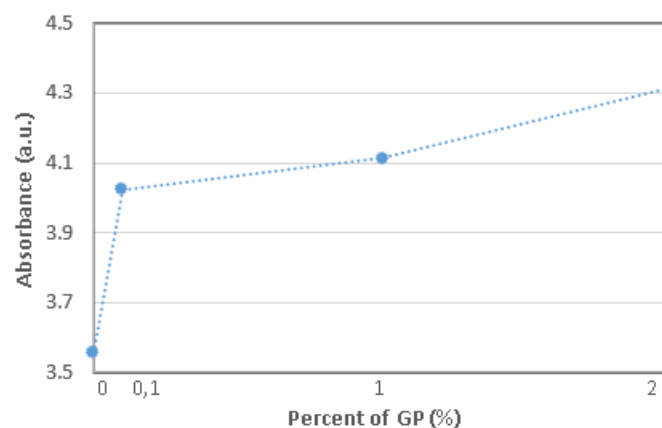


Figure 3.4- Relation between absorbance and crosslinking degree of the PDA coated membranes

3.3.2 Water contact angle measurements

The results of the WCA measurements, performed on the obtained membranes, are depicted on Figure 3.5. Due the presence of amino and acetamide groups (both polar)

CHT is considered a hydrophilic macromolecule³⁷. However, all the unmodified CHT membranes used in this work (blue bars) show an hydrophobic character. CHT, 0.1% crosslinked CHT, 1% crosslinked CHT and 2% crosslinked CHT membranes present a WCA around 100°, which could be related to their rougher morphology (see SEM and AFM sections). This finding is supported by similar results shown by Caridade and coworkers³⁸.

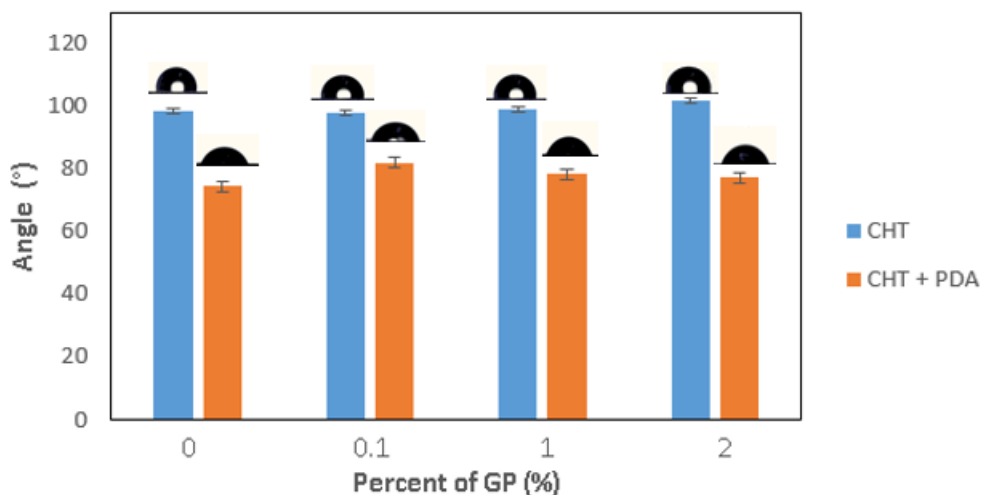


Figure 3.5- WCA measurements of unmodified (blue bars) and modified CHT membranes with PDA (orange bars).

Taking into account only the crosslinking effect, an increase of the WCA would be expected as the crosslinking degree increases, for the unmodified membranes. In fact, as GP reacts with CHT in the more hydrophilic groups (amines), it is expected that the crosslinking agent decreases the hydrophilicity of CHT, i.e., increase its hydrophobic character, however, this WCA increase was not verified. For the PDA modified membranes (Figure 4, orange bars), it was observed that the crosslinking degree did not have a strong influence on their wettability once their WCA is almost constant among all the studied conditions. However, a consistent decrease on the WCA to a value of $\sim 78^\circ$ was found when the unmodified membranes were compared with the modified ones. Such results suggested that the hydrophobicity of the membranes was counteracted when the membranes were modified with the PDA coating, rendering the membranes with a hydrophilic character. Other authors have observed a decrease in the WCA on PDA modified surfaces^{15,39}.

3.3.3 Scanning Electron Microscopy (SEM) and Atomic force microscopy (AFM)

The surface morphology of all the produced membranes was evaluated by SEM – see figure 3.6. It was observed that unmodified membranes present a rougher surface whereas PDA modified membranes presents a smoother surface. Particularly for unmodified CHT membranes (Figure 3.6 a) it was observed a rougher surface when compared with 0.1% crosslinked CHT, 1% crosslinked CHT and 2% crosslinked CHT.

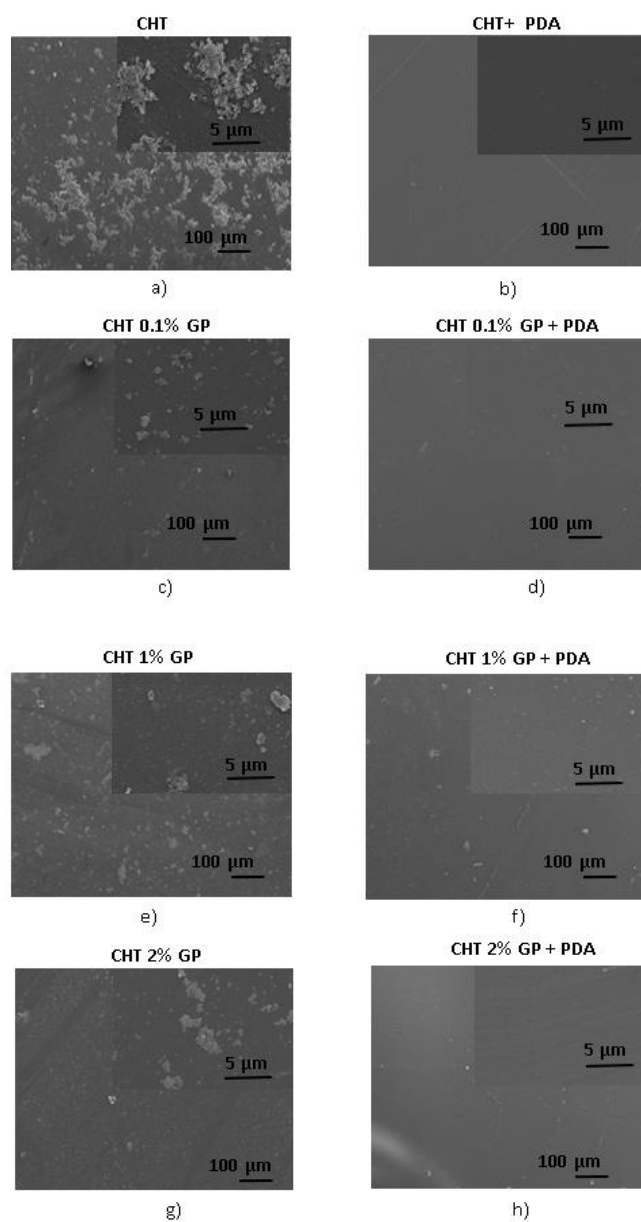
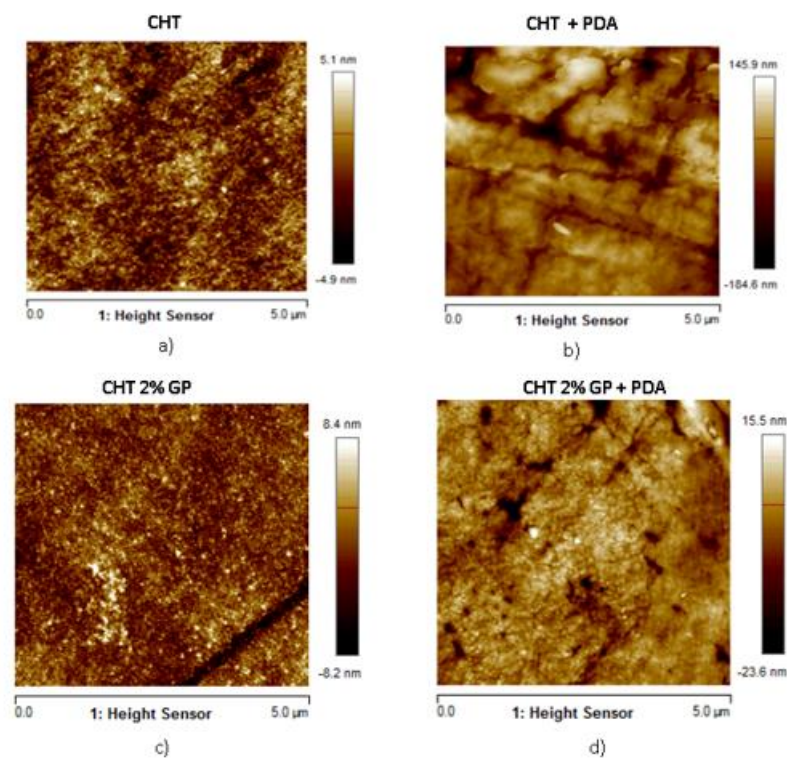


Figure 3.6- Representative SEM images of- a) CHT membranes; b) modified CHT membranes; c) 0.1% crosslinked CHT membranes; d) modified 0.1% crosslinked CHT membranes; e) 1% crosslinked CHT membranes; f) modified 1% crosslinked CHT membranes; g) 2% crosslinked CHT membranes and h) modified 2% crosslinked CHT membranes.

The roughness of both unmodified and modified membranes is shown in figure 3.7. By the observation of the captured 3D images, all membranes revealed some roughness and heterogeneity. Taking into account the AFM images and the root mean Square (R_q) and average roughness (R_a) values (shown in figure 3.7) it can be said that there are no significant changes in the roughness at the nanolevel for all the membranes. In figures 3.7b and 3.7d, the presence of small agglomerates were shown which corresponds to PDA.



	CHT	CHT + PDA	CHT 2% GP	CHT 2% GP + PDA
R_q (nm)	3.63 ± 2.57	3.03 ± 0.00	2.20 ± 0.16	4.72 ± 0.00
R_a (nm)	2.74 ± 1.89	2.37 ± 0.01	1.70 ± 0.17	3.23 ± 0.28

Figure 3.7- Representative AFM images ($5\mu\text{m} \times 5\mu\text{m}$) of- a) CHT membranes; b) modified CHT membranes; c) 2% crosslinked CHT membranes and d) modified 2% crosslinked CHT membranes. R_q and R_a values of the studied surfaces.

AFM tests coupled with nanoindentation tests were also performed in order to determine the adhesion force and the Young's modulus of both unmodified and modified 2 % crosslinked CHT membranes. Only the mechanical properties of the samples with

this composition were analysed as it was previously shown that the wettability of all the modified samples was nearly the same. The results are shown in Figure 3.8. It can be seen that the CHT 2% GP membranes were stiffer than the ones modified with PDA which means that the presence of the coating decreased the stiffness of the membranes. Oppositely, it was verified that the presence of polydopamine have a significant effect on the adhesive properties of the CHT 2% GP + DOP membranes, in agreement with previously reported data¹¹.

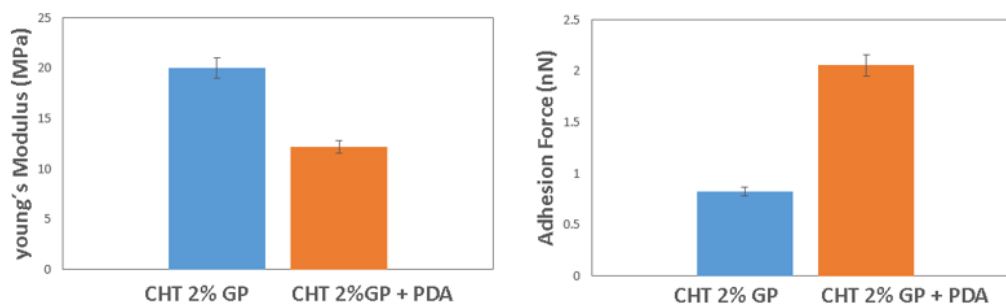


Figure 3.8- Young's Modulus and adhesion force of unmodified (blue bars) and modified (orange bars) 2% crosslinked CHT membranes determined by AFM.

3.3.4 Bioadhesion tests

Lap shear stress tests were performed on all the produced membranes, both unmodified and modified membranes, where each assembly was composed of pig skin/membranes, in order to measure the adhesion strength. It was observed, by naked eye, that all the formulations with the PDA coating exhibited some resistance to the detachment between the pig skin and the modified membranes. Moreover, the adhesion strength values were similar, independently of the crosslinking degree. Figure 3.9 presents the values for the 2% crosslinked membranes. It can be seen that the adhesion strength values were higher for the modified membranes as expected^{40,41}. Such results are in agreement with the ones obtained in the AFM section.

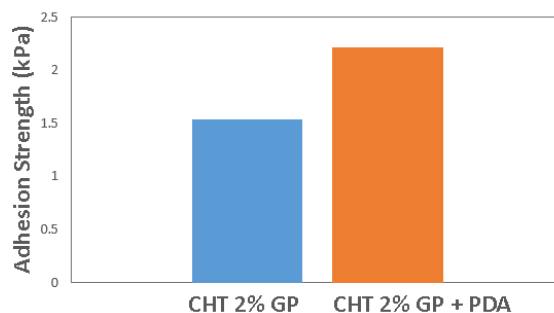


Figure 3.9- Bioadhesion tests performed according ASTM D1002: Adhesion strength for both unmodified (blue bars) and modified (orange bars) 2% crosslinked membranes.

3.4 Conclusions

In summary, we were able to modify CHT membranes crosslinked at several GP degrees by coating them with polydopamine. Firstly, the crosslinking degree was evaluated by UV-Vis experiments. The same technique was used to confirm the presence of polydopamine. By SEM experiments, it was verified that the morphology of the unmodified membranes was rougher than the modified by polydopamine. Such results were corroborated by WCA measurements. It was verified that the uncrosslinked and crosslinked CHT membranes show a hydrophobic character and after polydopamine coating the membranes became hydrophilic, even if crosslinked, confirming the success of the polydopamine coating. AFM experiments revealed that the presence of polydopamine leads to a decrease of the membranes stiffness, however the polydopamine coatings confer adhesive properties to the membranes both uncrosslinked and crosslinked. The properties of the bioadhesives herein reported seems to be promising biomaterials for skin regeneration applications.

References

1. Yamada, K. *et al.* Chitosan based water-resistant adhesive. Analogy to mussel glue. *Biomacromolecules* **1**, 252–258 (2000).
2. Lee, H., Scherer, N. F. & Messersmith, P. B. Single-molecule mechanics of mussel adhesion. *Proc. Natl. Acad. Sci. U. S. A.* **103**, 12999–13003 (2006).
3. Murphy, J. L., Vollenweider, L., Xu, F. & Lee, B. P. Adhesive performance of biomimetic adhesive-coated biologic scaffolds. *Biomacromolecules* **11**, 2976–2984 (2010).
4. Lee, B. P., Dalsin, J. L. & Messersmith, P. B. Synthesis and Gelation of DOPA-Modified Poly (ethylene glycol) Hydrogels. 1038–1047 (2002).
5. Dalsin, J. L., Hu, B. H., Lee, B. P. & Messersmith, P. B. Mussel adhesive protein mimetic polymers for the preparation of nonfouling surfaces. *J. Am. Chem. Soc.* **125**, 4253–4258 (2003).
6. Morgan, S. Polyphenolic Substance of *Mytilus edulis* : Novel. 4–6
7. Ku, S. H., Ryu, J., Hong, S. K., Lee, H. & Park, C. B. General functionalization route for cell adhesion on non-wetting surfaces. *Biomaterials* **31**, 2535–2541 (2010).
8. Charlot, A. *et al.* All-in-one strategy for the fabrication of antimicrobial biomimetic films on stainless steel. *J. Mater. Chem.* **19**, 4117 (2009).
9. Wei, Q., Zhang, F., Li, J., Li, B. & Zhao, C. Oxidant-induced dopamine polymerization for multifunctional coatings. *Polym. Chem.* **1**, 1430 (2010).
10. Zhou, P. *et al.* Rapidly-Deposited Polydopamine Coating via High Temperature and Vigorous Stirring: Formation, Characterization and Biofunctional Evaluation. *PLoS One* **9**, e113087 (2014).
11. Guardingo, M. *et al.* Bioinspired Catechol-Terminated Self-Assembled Monolayers with Enhanced Adhesion Properties. *Small* **10**, 1594–1602 (2013).
12. Lee, H., Rho, J. & Messersmith, P. B. Facile conjugation of biomolecules onto surfaces via mussel adhesive protein inspired coatings. *Adv. Mater.* **21**, 431–434 (2009).
13. Ryu, J. H. *et al.* Catechol-functionalized chitosan/pluronic hydrogels for tissue adhesives and hemostatic materials. *Biomacromolecules* **12**, 2653–2659 (2011).
14. Cui, J. *et al.* Immobilization and intracellular delivery of an anticancer drug using mussel-inspired polydopamine capsules. *Biomacromolecules* **13**, 2225–2228 (2012).

15. Yang, F. K. & Zhao, B. Adhesion Properties of Self-Polymerized Dopamine Thin Film. *Open Surf. Sci. J.* **3**, 115–122 (2011).
16. Lee, H., Dellatore, S. M., Miller, W. M. & Messersmith, P. B. Mussel-inspired surface chemistry for multifunctional coatings. *Science* **318**, 426–430 (2007).
17. Tsai, W. B., Chen, W. T., Chien, H. W., Kuo, W. H. & Wang, M. J. Poly(dopamine) coating of scaffolds for articular cartilage tissue engineering. *Acta Biomater.* **7**, 4187–4194 (2011).
18. Yang, S. H. *et al.* PDA33-Mussel-inspired encapsulation and functionalization of individual yeast cells. *J. Am. Chem. Soc.* **133**, 2795–2797 (2011).
19. Lee, H., Lee, B. P. & Messersmith, P. B. A reversible wet/dry adhesive inspired by mussels and geckos. *Nature* **448**, 338–341 (2007).
20. Bansal, V., Sharma, P. K., Sharma, N., Pal, O. P. & Malviya, R. Applications of Chitosan and Chitosan Derivatives in Drug Delivery. *Biol. Res.* **5**, 28–37 (2011).
21. Croisier, F. & Jérôme, C. Chitosan-based biomaterials for tissue engineering. *Eur. Polym. J.* **49**, 780–792 (2013).
22. Rinaudo, M. Chitin and chitosan: Properties and applications. *Progress in Polymer Science* **31**, 603–632 (2006).
23. Mourya, V. K. & Inamdar, N. N. Chitosan-modifications and applications: Opportunities galore. *React. Funct. Polym.* **68**, 1013–1051 (2008).
24. Ravi Kumar, M. N. . A review of chitin and chitosan applications. *Reactive and Functional Polymers* **46**, 1–27 (2000).
25. Jin, J., Song, M. & Hourston, D. J. Novel chitosan-based films cross-linked by genipin with improved physical properties. *Biomacromolecules* **5**, 162–168 (2004).
26. Chiono, V. *et al.* Genipin-crosslinked chitosan/gelatin blends for biomedical applications. *J. Mater. Sci. Mater. Med.* **19**, 889–898 (2008).
27. Caridade, S. G., da Silva, R. M. P., Reis, R. L. & Mano, J. F. Effect of solvent-dependent viscoelastic properties of chitosan membranes on the permeation of 2-phenylethanol. *Carbohydr. Polym.* **75**, 651–659 (2009).
28. Muzzarelli, R. A. A. Genipin-crosslinked chitosan hydrogels as biomedical and pharmaceutical aids. *Carbohydrate Polymers* **77**, 1–9 Genipin, a crystalline and well defined chemica (2009).
29. Artech Pujana, M., Pérez-Álvarez, L., Cesteros Iturbe, L. C. & Katime, I. Biodegradable chitosan nanogels crosslinked with genipin. *Carbohydr. Polym.* **94**, 836–842 (2013).

30. Xu, J., Soliman, G. M., Barralet, J. & Cerruti, M. Mollusk glue inspired mucoadhesives for biomedical applications. *Langmuir* **28**, 14010–14017 (2012).
31. Lim, S., Choi, Y. S., Kang, D. G., Song, Y. H. & Cha, H. J. The adhesive properties of coacervated recombinant hybrid mussel adhesive proteins. *Biomaterials* **31**, 3715–3722 (2010).
32. V. Sencadas, D.M. Correia, A. Areias, G. Botelho, A.M. Fonseca, I.C. Neves, J.L. Gómez-Ribelles, S. L. M. Determination of the parameters affecting electrospun chitosan fiber size distribution and morphology. *Carbohydr. Polym.* **87**, 1295–1301 (2012).
33. M. Terbojevich, A. Cosani, R. A. A. M. Molecular parameters of chitosans depolymerized with the aid of papain. *Carbohydr. Polym* **29**, 63 (1996).
34. Harris, R., Lecumberri, E. & Heras, A. Chitosan-Genipin Microspheres for the Controlled Release of Drugs: Clarithromycin, Tramadol and Heparin. *Mar. Drugs* **8**, 1750–1762 (2010).
35. Butler, M. F., Ng, Y. F. & Pudney, P. D. A. Mechanism and kinetics of the crosslinking reaction between biopolymers containing primary amine groups and genipin. *J. Polym. Sci. Part A Polym. Chem.* **41**, 3941–3953 (2003).
36. Huang, S. *et al.* Complexes of polydopamine-modified clay and ferric ions as the framework for pollutant-absorbing supramolecular hydrogels. *Langmuir* **29**, 1238–1244 (2013).
37. Assis, O. B. G. Alteração do caráter hidrofílico de filmes de quitosana por tratamento de plasma de HMDS. *Quim. Nov.* **33**, 603–606 (2010).
38. Caridade, S. G. *et al.* Chitosan membranes containing micro or nano-size bioactive glass particles: Evolution of biomineralization followed by in situ dynamic mechanical analysis. *J. Mech. Behav. Biomed. Mater.* **20**, 173–183 (2013).
39. Jiang, Jin-Hong, Li Ping Zhu, Hong-Tao Zhang, Bao-Ku Zhu, Y.-Y. X. Improved hydrodynamic permeability and antifouling properties of poly(vinylidene fluoride) membranes using polydopamine nanoparticles as additives. *J. Memb. Sci.* **457**, 73–81 (2014).
40. Anderson, T. H. *et al.* The contribution of DOPA to substrate-peptide adhesion and internal cohesion of mussel-inspired synthetic peptide films. *Adv. Funct. Mater.* **20**, 4196–4205 (2010).
41. Brubaker, C. E. & Messersmith, P. B. Enzymatically degradable mussel-inspired adhesive hydrogel. *Biomacromolecules* **12**, 4326–34 (2011).

Chapter 4 - Concluding remarks

There has been a continuous progress in the synthesis of new materials based on natural products, in an attempt to replace synthetic materials currently in use, in different areas. The most interesting advantage of natural biomaterials is their abundance and ecofriendly nature. Especially in biomedical field, biopolymers have favorable features in comparison to synthetic polymers, such as biocompatibility and biodegradability.

Inspired by nature, uncrosslinked and crosslinked CHT membranes were successfully produced by solvent casting, and afterwards coated with dopamine, a biomolecule able to mimic the adhesive component, DOPA, of marine mussels. The coatings were successfully achieved once dopamine formed a self-polymerized coating in both uncrosslinked and crosslinked CHT membranes.

It was verified that dopamine improves the adhesive properties of the membranes, and also give them a hydrophilic character. As it is intend to use such bioadhesives membranes on skin regeneration applications its hydrophilic character is an essential requirement.

In future work, it would be important to study the adhesion properties of such membranes in more detail. Moreover, the biological behavior of skin cells on the membranes will need to be evaluated.

Annex

Calculation of the degree of deacetylation

As mentioned earlier in Chapter 2, the degree of deacetylation (DD) of the CHT powder that was purified by a recrystallization process was determined by H-NMR. The DD of the purified CHT powder was calculated through the following formula:

$$DD (\%) = \frac{H_1D}{H_1D + \left(\frac{Hac}{3}\right)} \times 100$$

Where H_1D is referent to the deacetylated group proton and Hac is referent to the acetyl group proton. In figure 1 the H-NMR spectrum obtained for our purified CHT powder is presented.

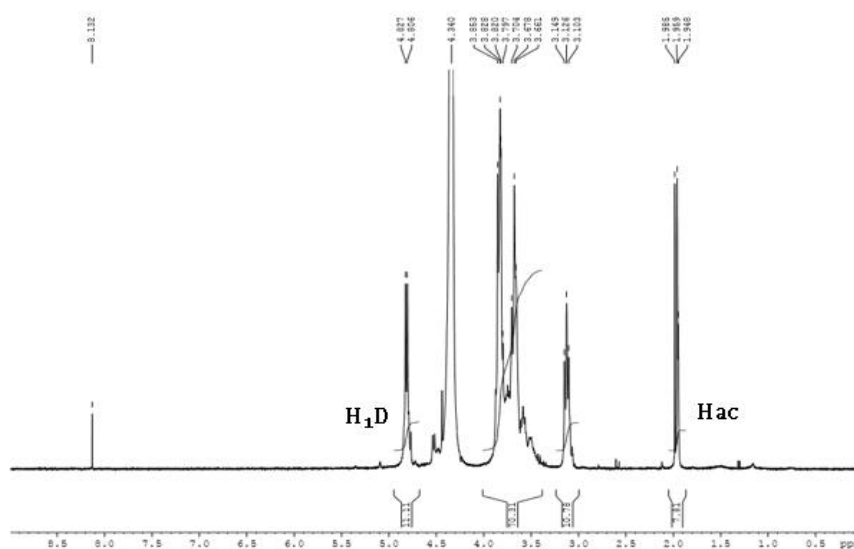


Figure 1- H-NMR spectrum of the purified chitosan.

$$DD (\%) = \frac{H_1D}{H_1D + \left(\frac{Hac}{3}\right)} \times 100 \Leftrightarrow DD (\%) = \frac{11.11}{11.11 + \left(\frac{7.81}{3}\right)} \times 100 = 81\%$$

Fourier Transform Infrared Spectrophotometry (FTIR)

As mentioned in Chapter 2, it was not possible to prove the presence of polydopamine through FTIR analysis, since there was no detection of any new band characteristic of polydopamine, as can be verified in figures 2, 3, 4 and 5.

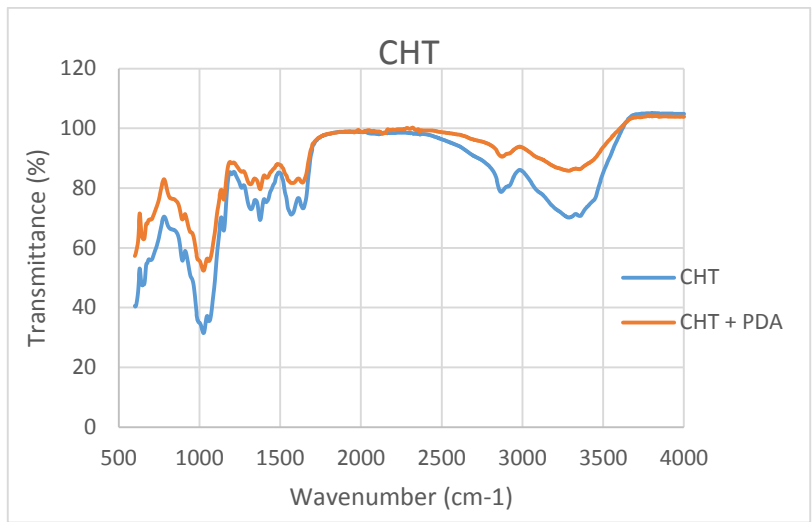


Figure 2- FTIR spectrum of the coated and uncoated chitosan film.

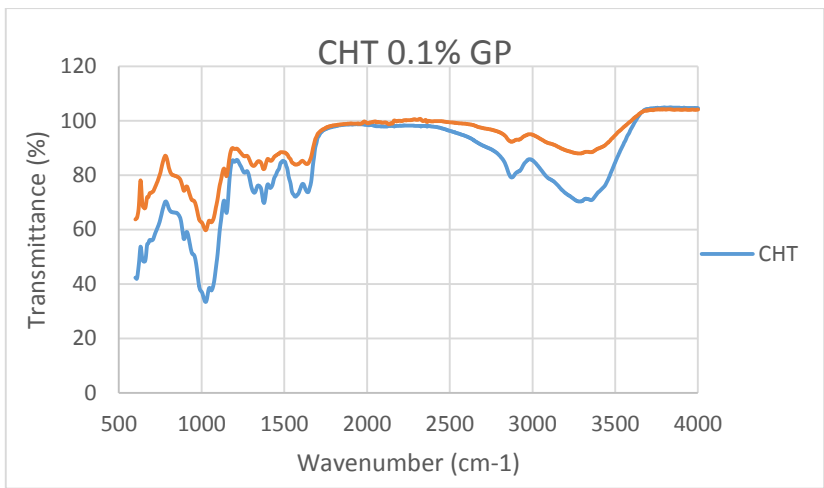


Figure 3- FTIR spectrum of coated and uncoated chitosan film 0.1% crosslinked.

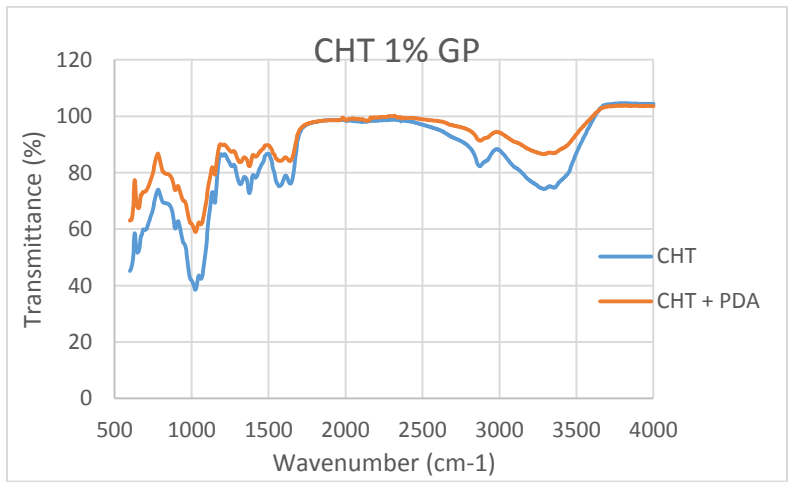


Figure 4- FTIR spectrum of coated and uncoated chitosan film 1% crosslinked.

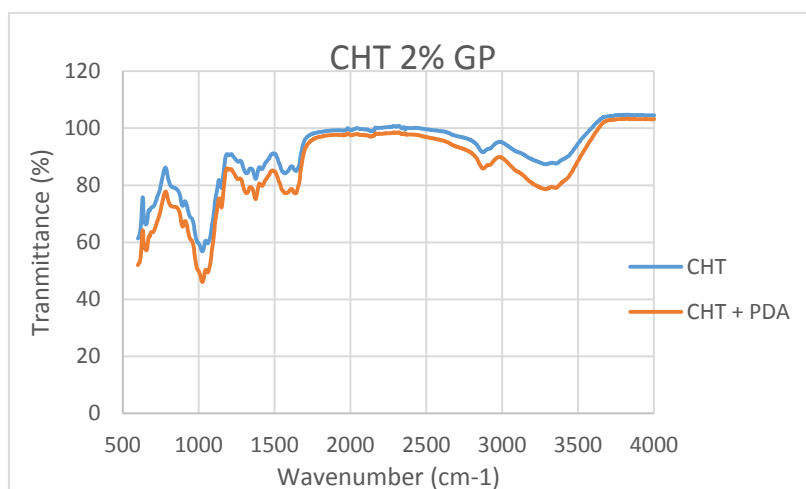


Figure 5- FTIR spectrum of coated and uncoated chitosan film 2% crosslinked.

Additionally, coated chitosan membranes were purposely left exposed to ambient light for 60 days. The WCA were measured again and it was found that when exposed to light the coated membranes lose their hydrophilic character and acquired a hydrophobic character. This finding could evidence some instability of the polydopamine coating performed under chitosan membranes. For this reason, further improvement of this coating strategy should be made.

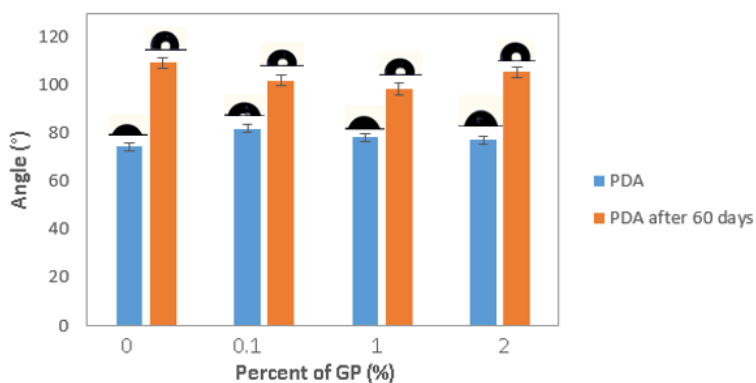


Figure 6- Contact angle of polydopamine coated membranes at starting time (blue bars) and polydopamine coated membranes after 60 days (orange bars).